Dark matter on small scales where are we with dSph galaxies?

Sizes

Ages/Chemical abundances/first stars

Kinematics

masses

Galaxy-scale Challenges for CDM

- On galaxy scales there is an opportunity to learn some (astro)physics:
  - Large galaxies of old stars, small galaxies of young (plus old) stars →‘downsizing’
  - Massive pure-thin-disk galaxies are very common: None should exist since mergers heat and puff-up disks, create bulges
  - The MWG has a thick disk, (GG&Reid 1983) and these stars are old, as in the bulge. This seems common but implies little merging since early times, to build them up
  - Sgr dSph (Ibata, GG & Irwin 1995) in the MWG proves late minor merging happens, but is clearly not dominant process in evolution of MWG except the outer halo, $R_{GC} > 25$ kpc
  - The ‘feedback’ requirement: otherwise gas cools and stars form too efficiently, plus angular momentum transported away from gas in mergers: stellar disks are too massive and compact
  - The substructure problem – how to hide them?

`Things` HI/Spitzer/Galex survey – cusped DM is very hard to find!

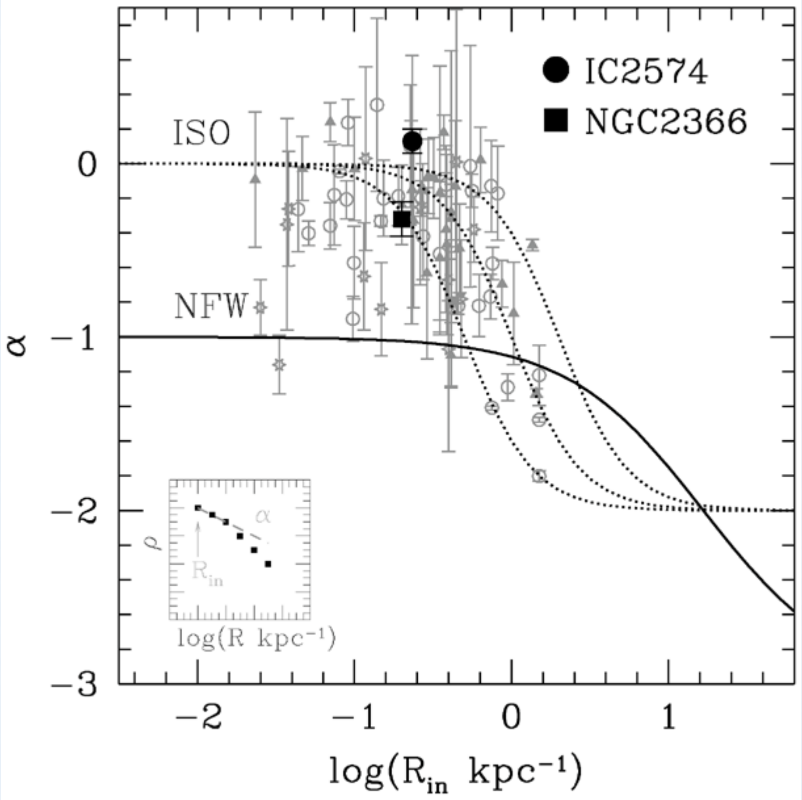

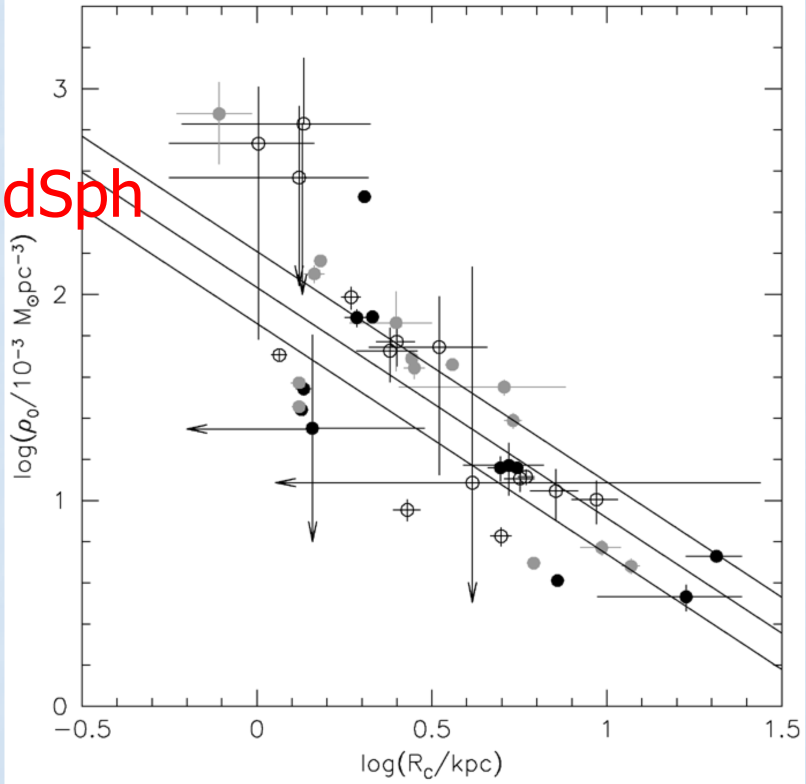

Oh etal; de Blok etal AJ 2008 v136 2761; 2648

Why go to the dSph to analyses CDM?

- In the Galactic disk the absence of dark matter maybe a puzzle – no accreted dwarfs?
- the local mass determination by Kuijken & Gilmore 1989,1991 remains the only experimental determination of (no) local DM– the same data are often reanalysed

CDM predicts many more satellite haloes than observed galaxies, at all masses (Moore et al 1999)

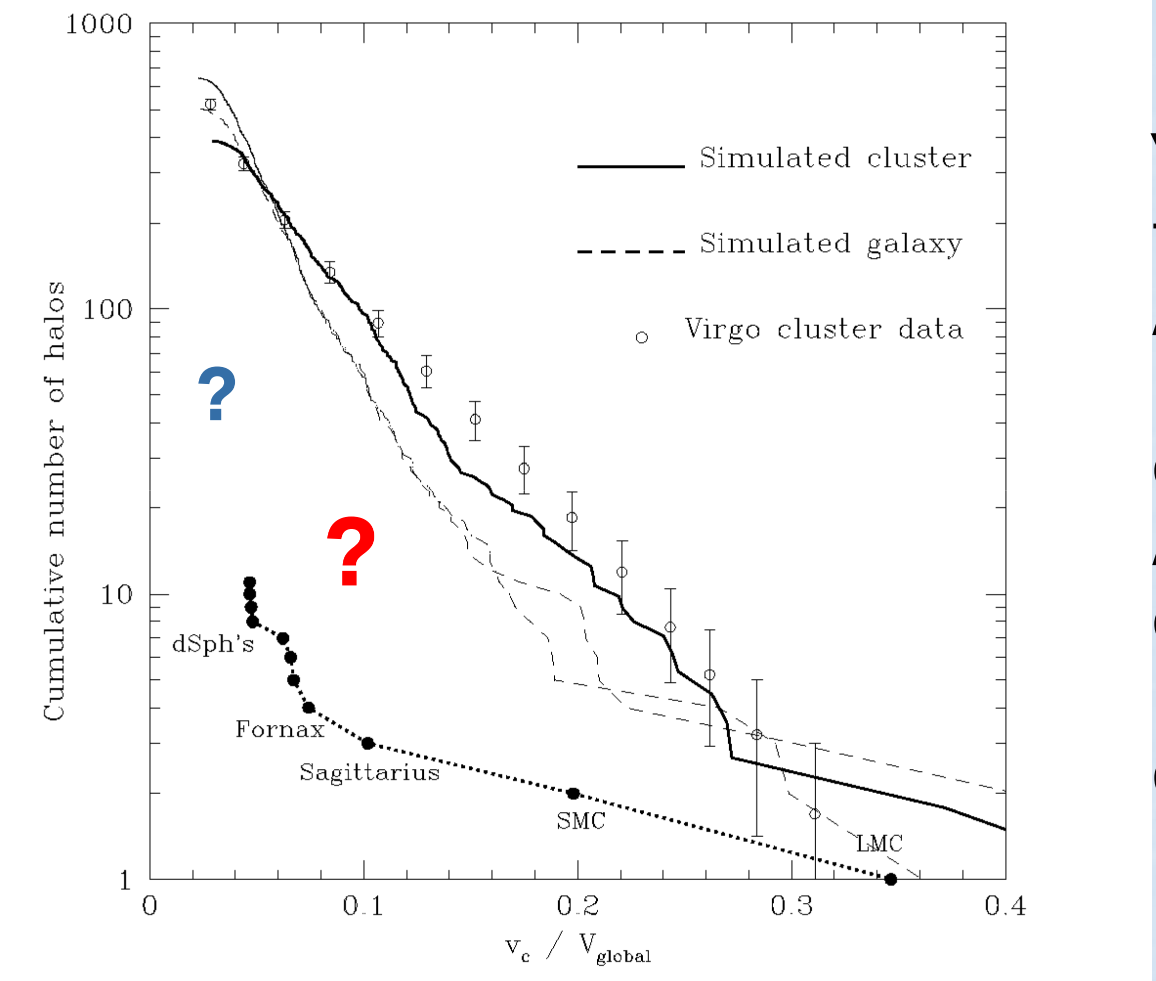

Use mass-dependent fixes, "feedback" to adjust mass function to luminosity.
At low masses we can limit maximum feedback from chemistry data.
At very low masses no gas cooling➔ no stars?
Limits there from [lack of] disk destruction.
But what is Vc for a dSph?

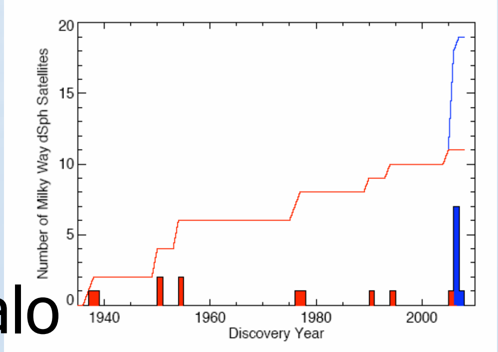

? Are there very many faint massive halos?

? Are there very,very many empty low-mass halo

Governato et al 2010

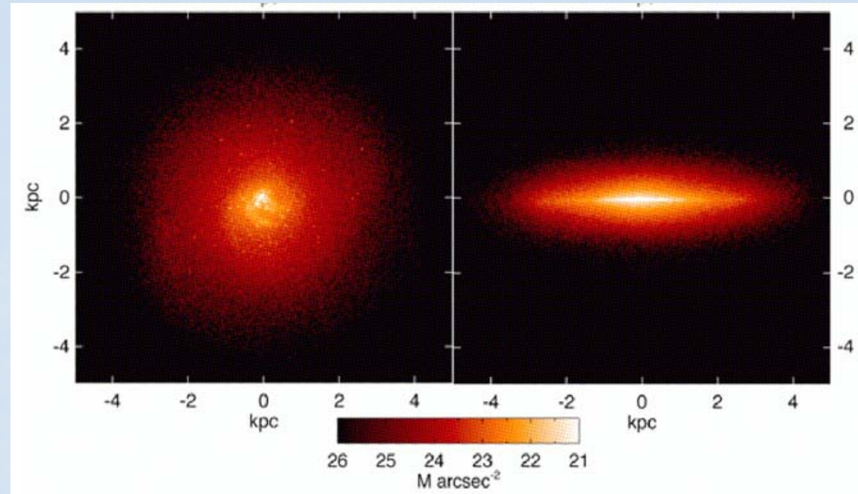

Three fainter discoveries from SDSS (Belokurov et al, 06a) – all required confirmation with deeper imaging, then spectroscopy

dSph d=45kpc

dSph d=150kpc

glob (?) d=25kpc

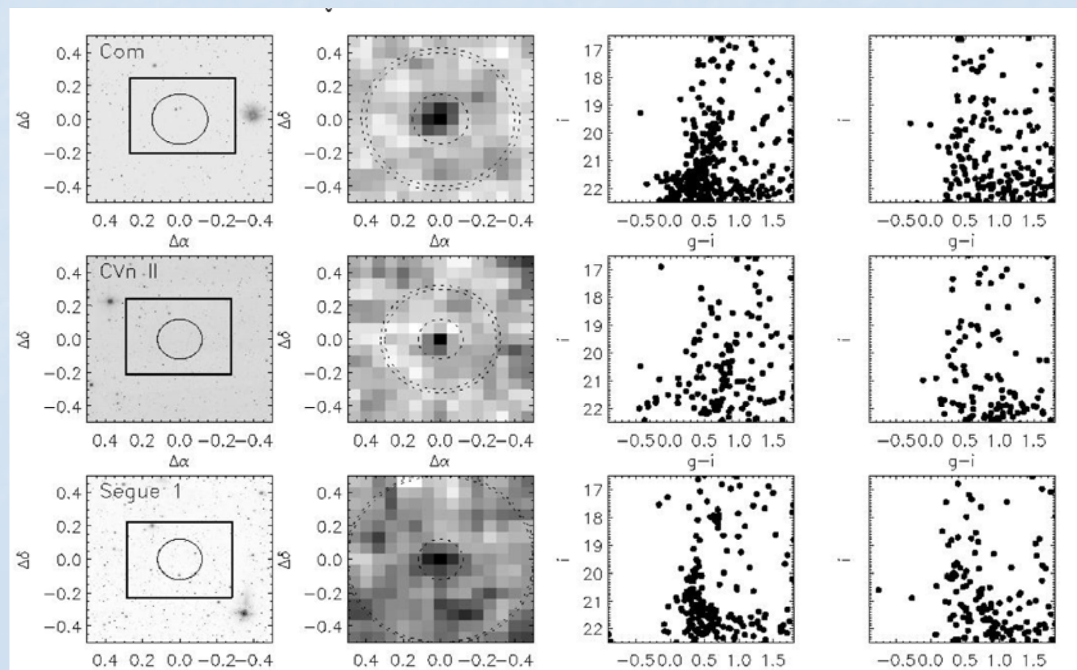

Field of Streams - updated

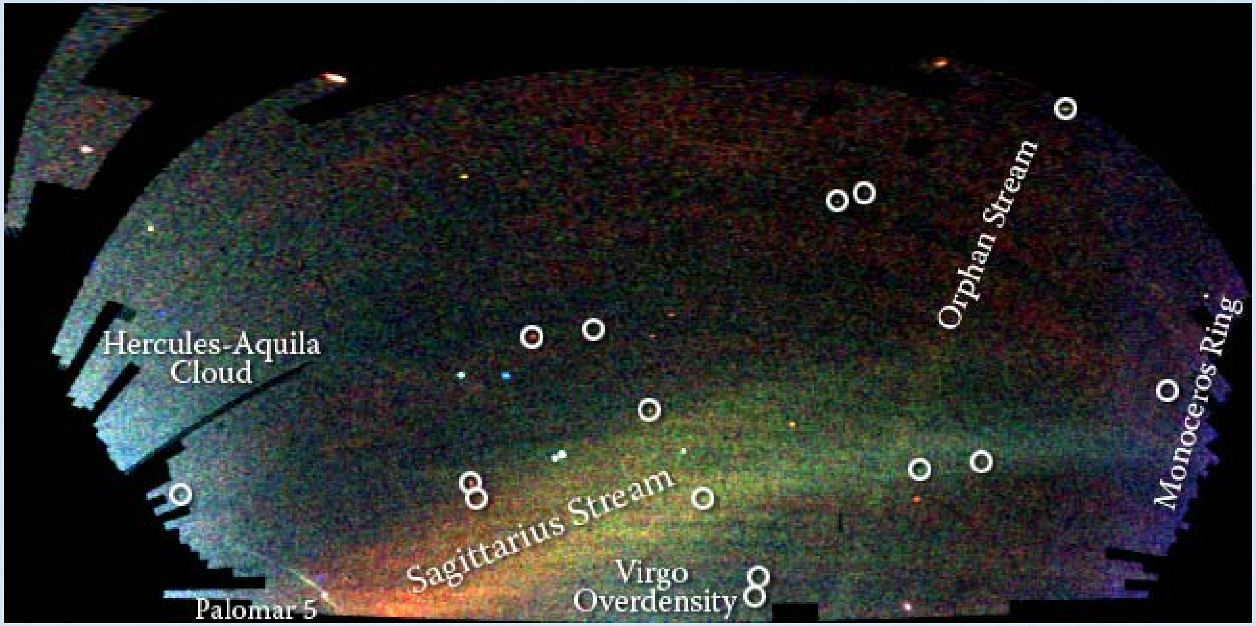

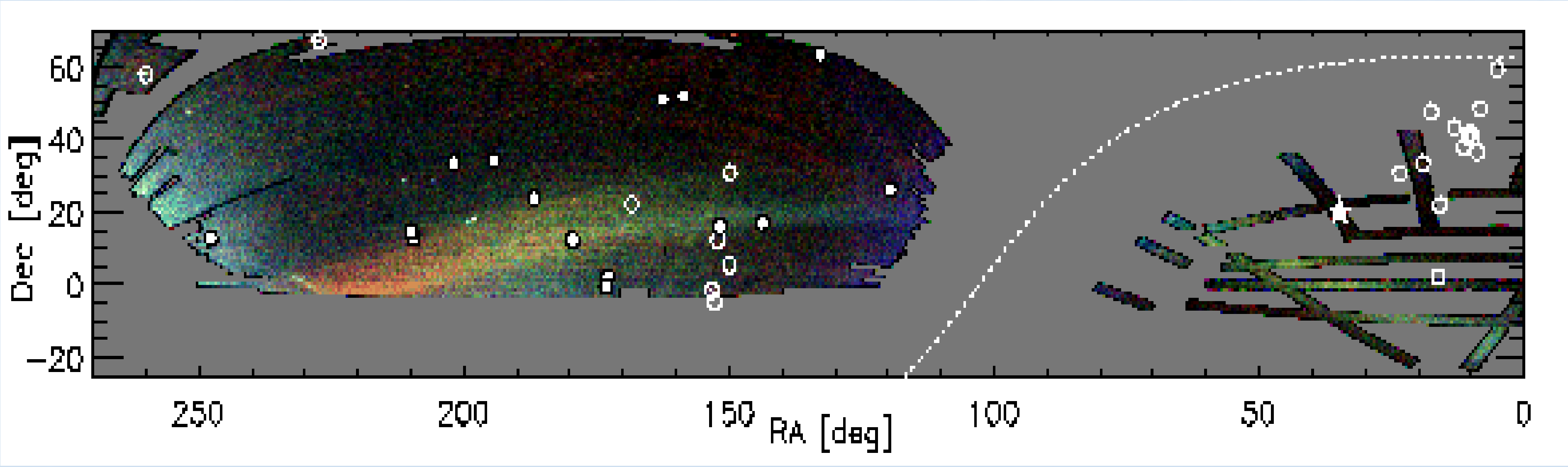

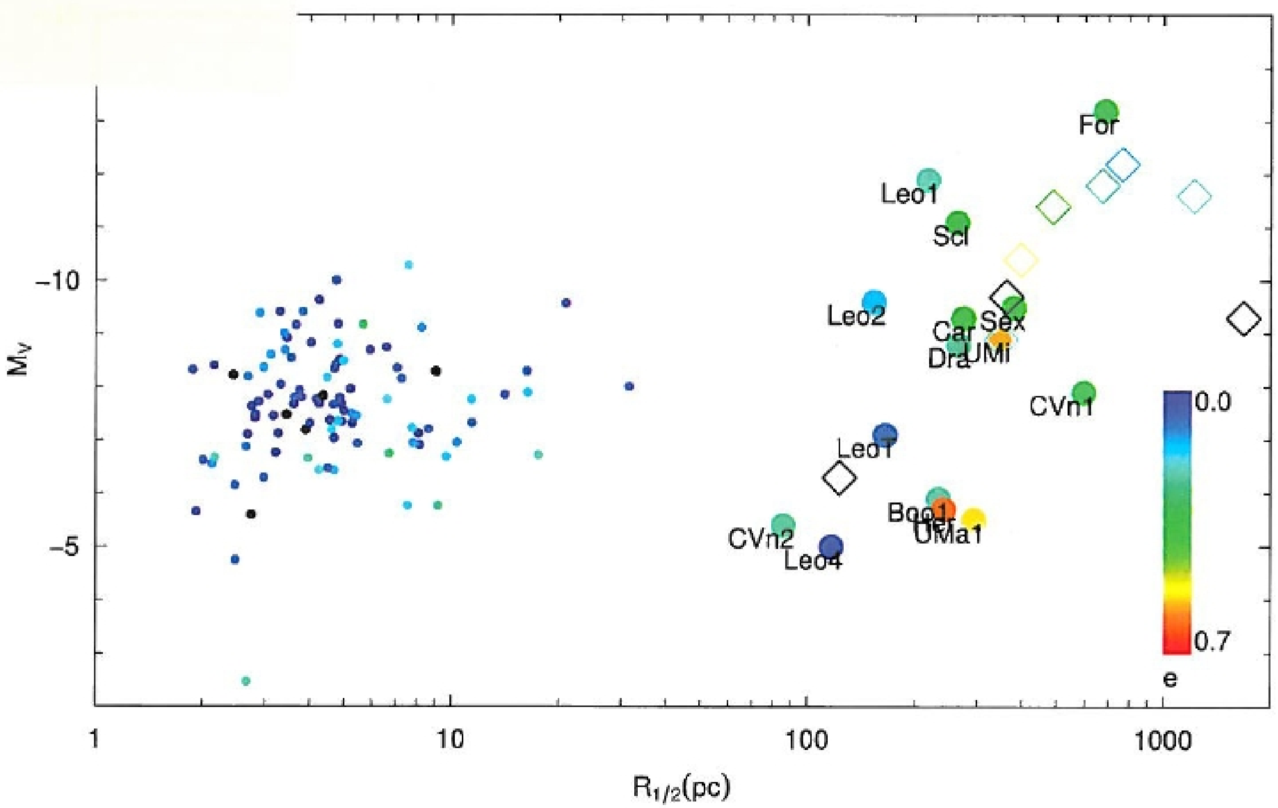

Figure 5.1 The distribution of Galactic and M31 dSphs and Galactic globular clusters in the logarithmic $r_{1/2}$ versus M_V plane. Galactic classical dSph and UFDs are plotted as coloured circles according to their ellipticities. The M31 dSphs and Galactic globular clusters are plotted as open diamonds and dots, respectively.

$10^9 L_\odot$

$10^7 L_\odot$

$10^3 L_\odot$

es

Update

Add ~20 new satellites, galaxies and star clusters - but note low yield from Southern SEGUE/SDSS imaging : only Segue 2 and Pisces II as candidate galaxies (Belokurov et al 09,10)

Chemical elements

- element production is very sensitive to SN progenitor initial stellar mass
- ➔ do we see a big scatter from single SNe?
- Metallicity DF defines length and time scale of SNe enrichment, and KE energy feedback/gas loss
- Do we see (near) zero abundances?
- If not, what pre-enriched the first halos? Did this same process affect Ly-alpha clouds?

Elemental Abundances: beyond metallicity

Alpha element and iron

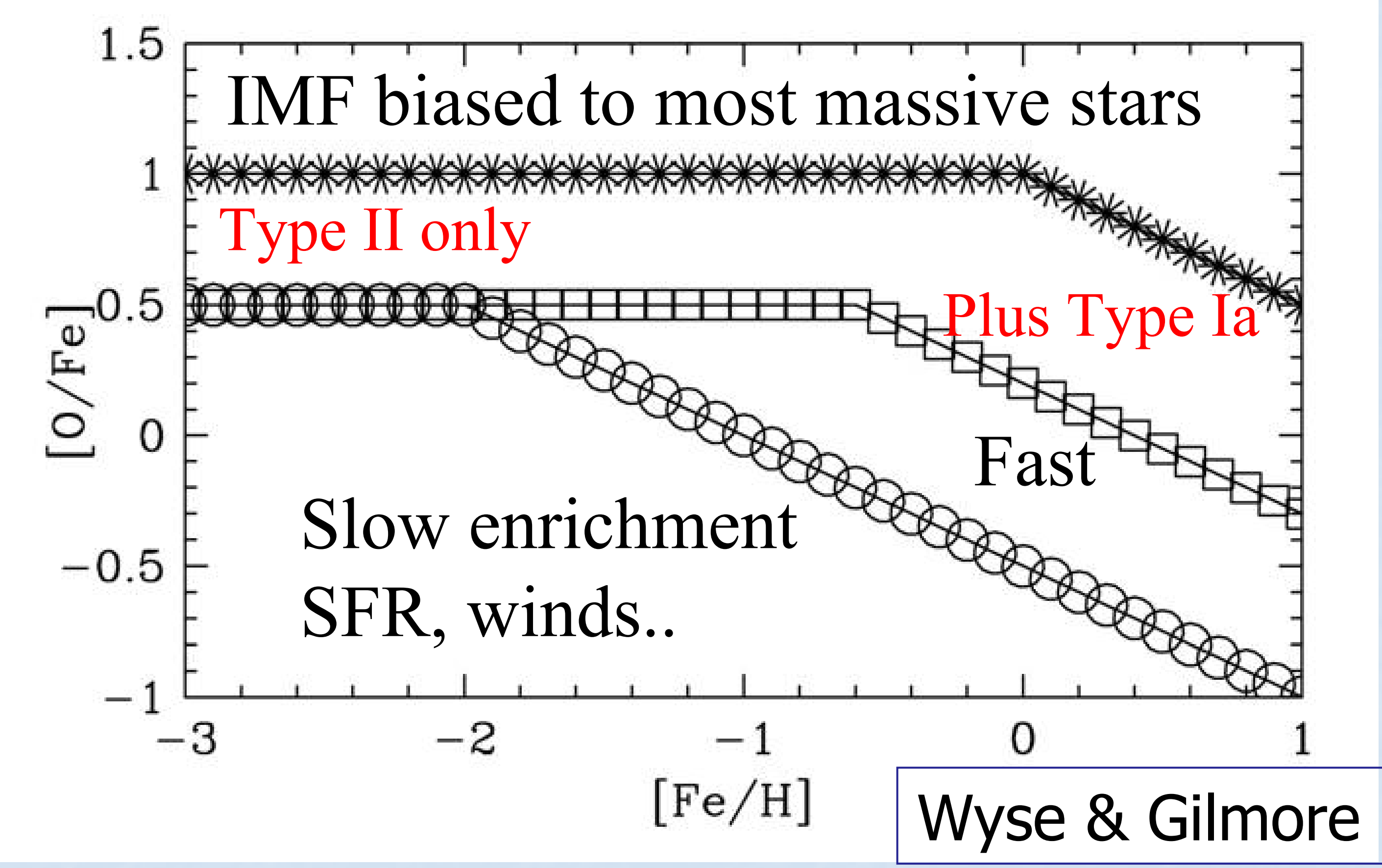

Wyse & Gilmore 1993

Self-enriched star forming region.

Assume good mixing so IMF-average yields

Core-collapse SNe α/Fe yields depend on progenitor stellar mass → IMF dependence

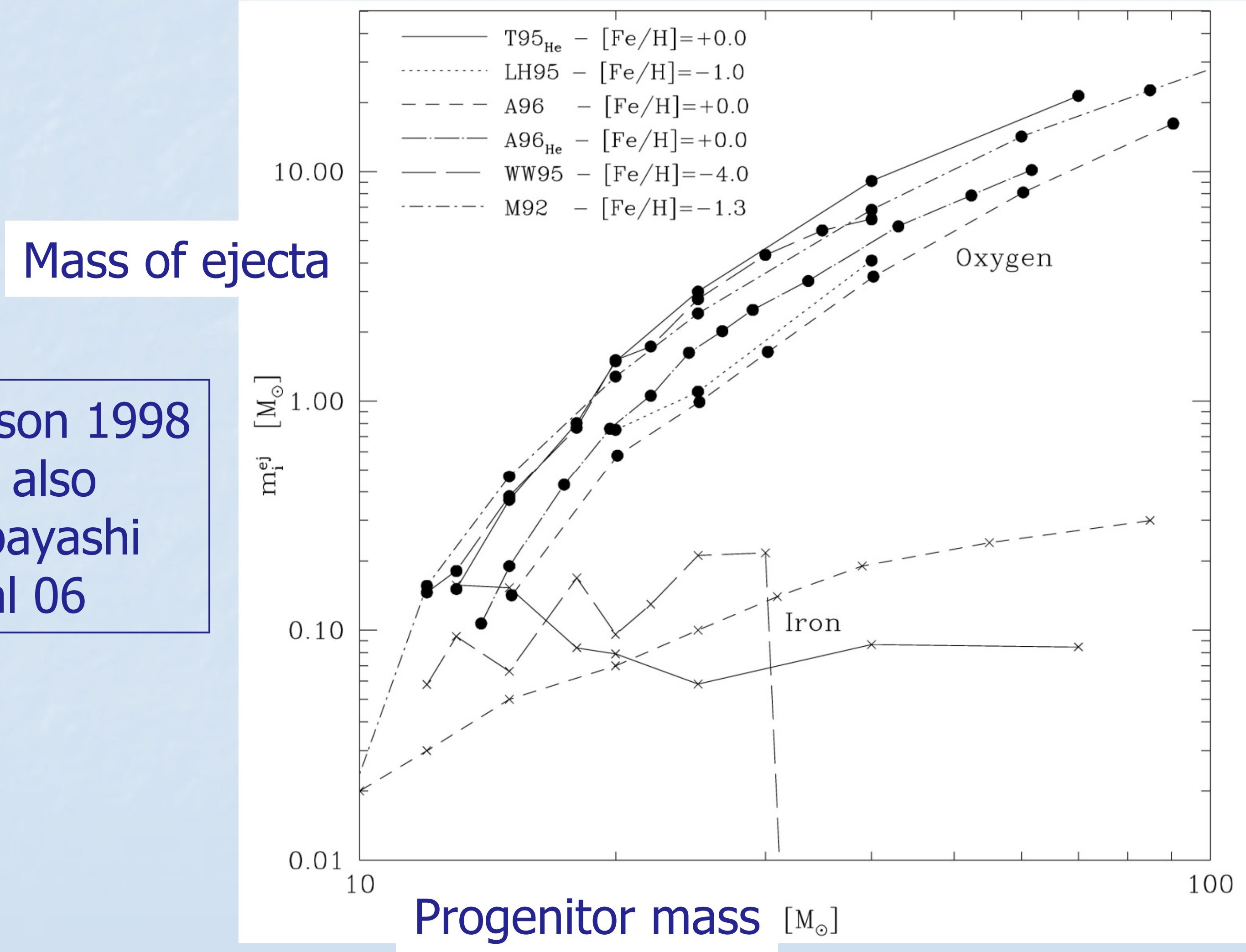

Gibson 1998
see also
Kobayashi
et al 06

Ruchti et al 2010

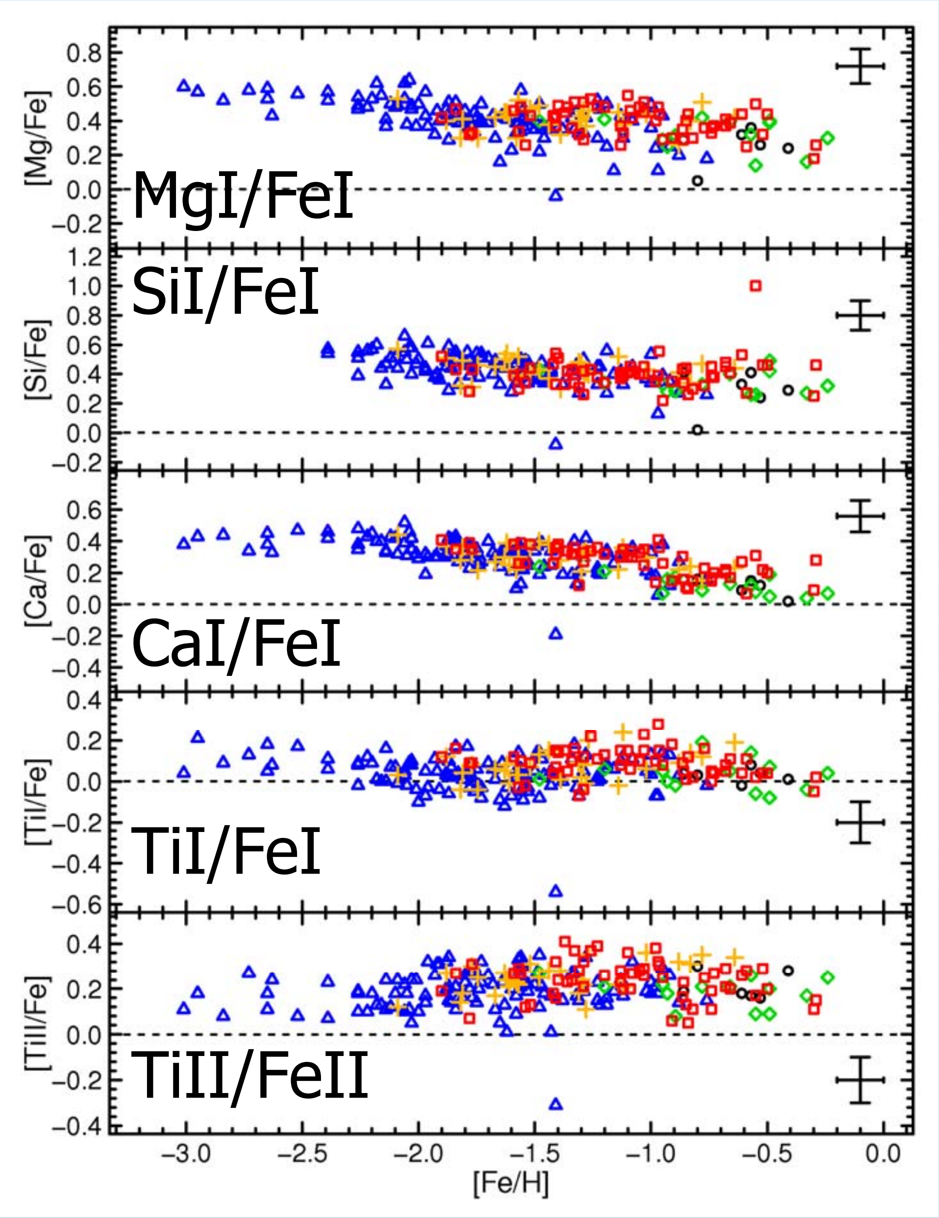

- Derived ratios of several key α-elements to iron, for 215 red giants

Blue = Halo

Red = Thick Disk

Black = Thin Disk

Orange = Thick/Halo

Green = Thin/Thick

➔galactic field stars all see a mass-average yield, which is spatially well mixed.

dSphs vs. MWG abundances

halo/thick disk is not the dSph graveyard

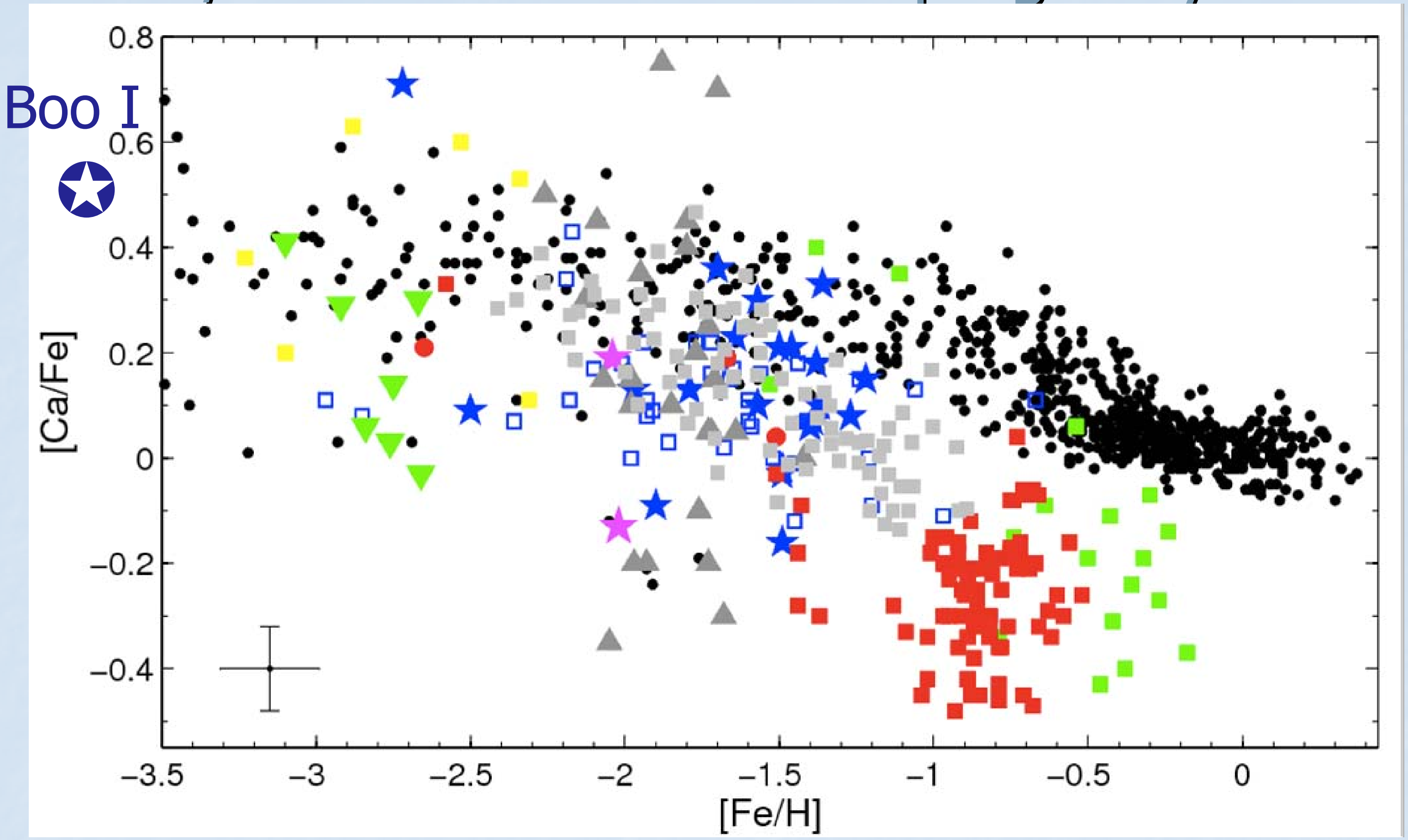

Shetrone et al. (2001, 2003): 5 dSphs
Sadakane et al. (2004): Ursa Minor
Monaco et al. (2005): Sagittarius
Koch et al. (2006, 2007): Carina
Letarte (2006): Fornax

Koch et al. (2008): Hercules
Shetrone et al. (2008): Leo II
Frebel et al. (2009): Coma Ber, Ursa Major
Aoki et al. (2009): Sextans
Hill et al. (in prep): Sculptor

Metallicity – luminosity relation revisited

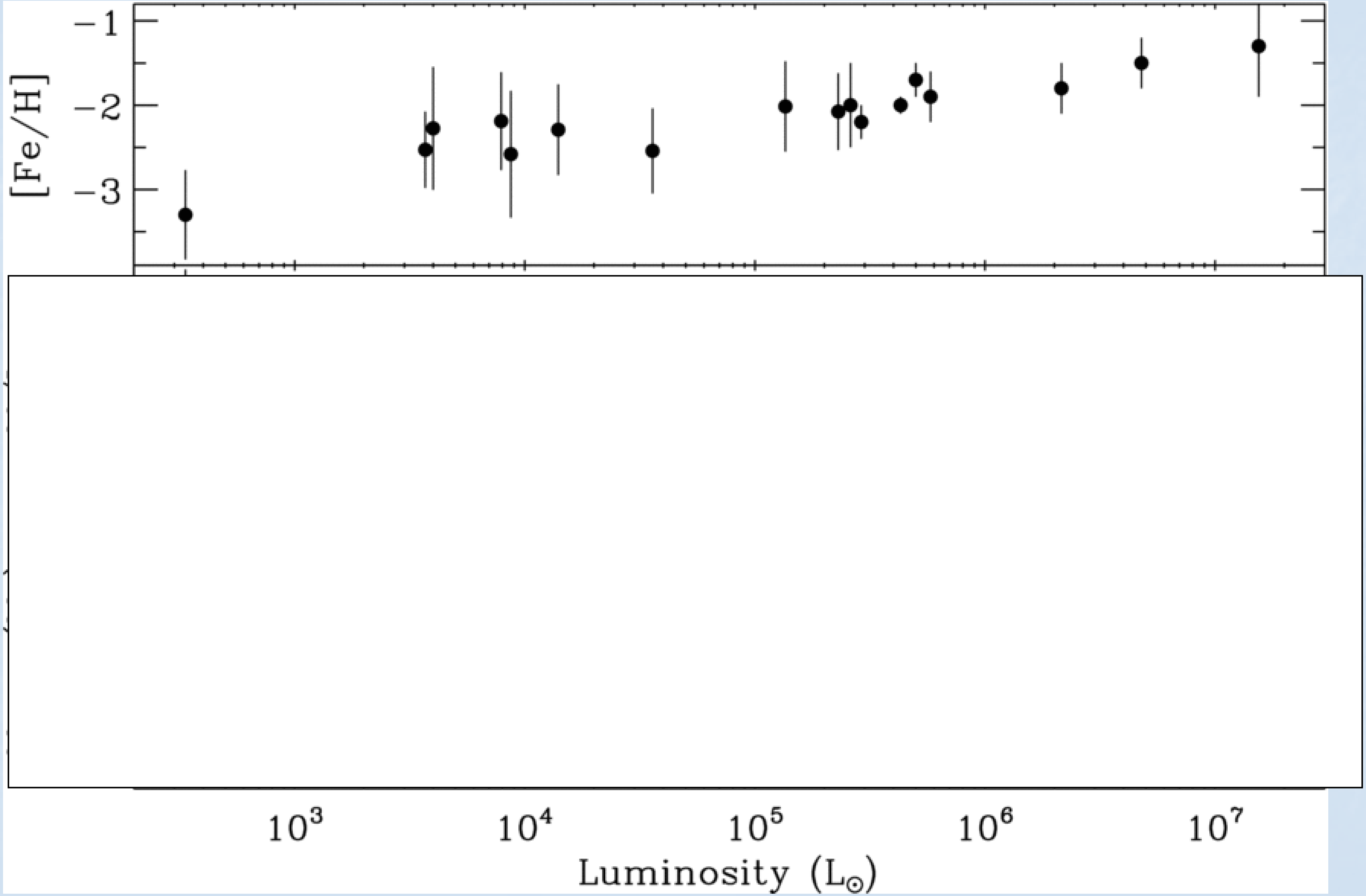

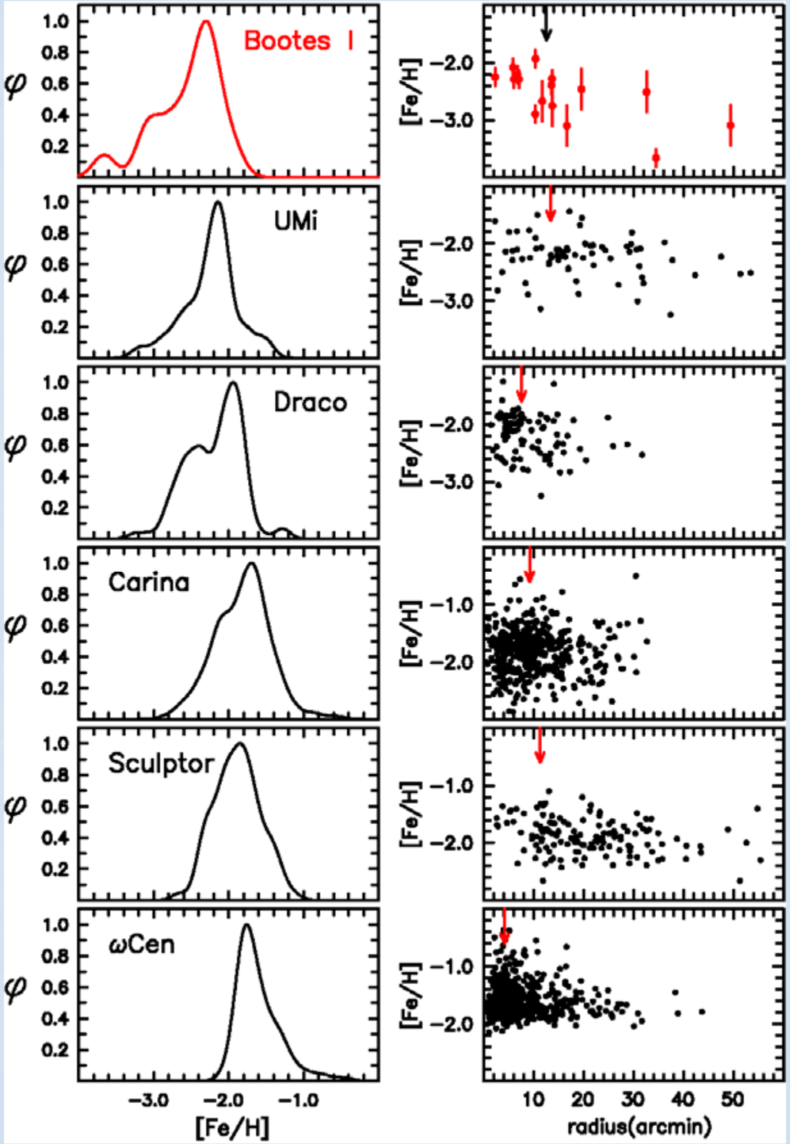

MDF data for Segue1	
Star	[Fe/H]
Geha et al	-3.3
7	-3.6
31	-1.9
71	-2.4
Same range as Bootes I	

dSph, including Bootes I, are not well-described by simple closed-box model. Star formation more likely episodic.

In Bootes I and Segue 1, Dark Matter most likely probably provides the deep potential well that prevents the ejecta of SNe from leaving the system.

Norris, Gilmore, etal in press

Chemical abundances:

Norris, GG et al 2010a

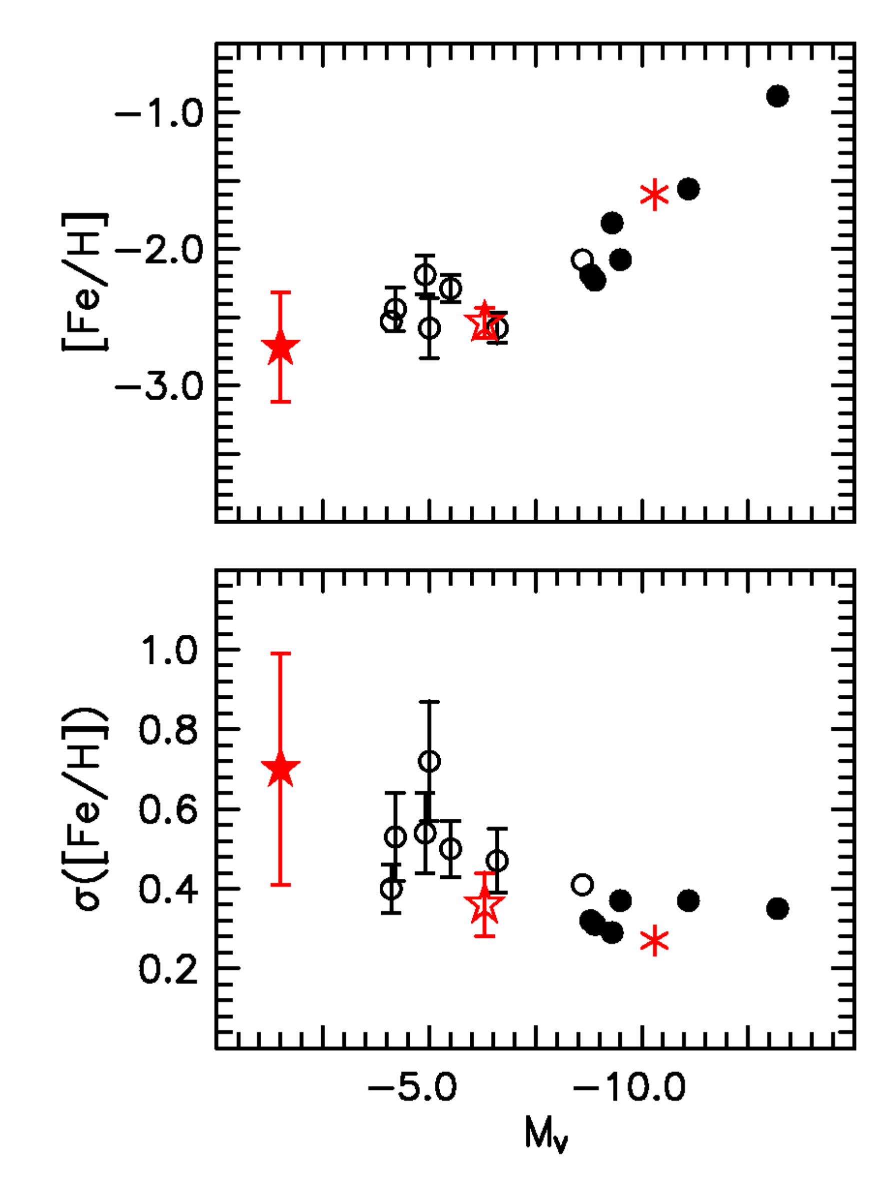

Mean iron abundance of member stars against total luminosity of host system: clear trend, hard to maintain if significant tidal stripping of host ➔ are any of the dSph tidally stripped?
➔ Interesting? since cusps survive, but cores don't in simulations.

Segue 1 (filled red star) based on only 4 stars – caution!

Dispersion in metallicity increases as luminosity decreases – consistent with inhomogeneous stochastic enrichment in low-mass halos, gentle feedback:
Highly variable SFR models predict high element **<u>ratio</u>** scatter

Topical chemical evolution models: lots more detail, but the same essential physics as simple model.
Key goal 1– limit star formation history & feedback on DM
Key goal 2 – relate the dSph to the Galaxy: building blocks?

Big challenge:
Understand the DF of metal-poor stars

What created the elements at low abundances?
Where are the ancestors?

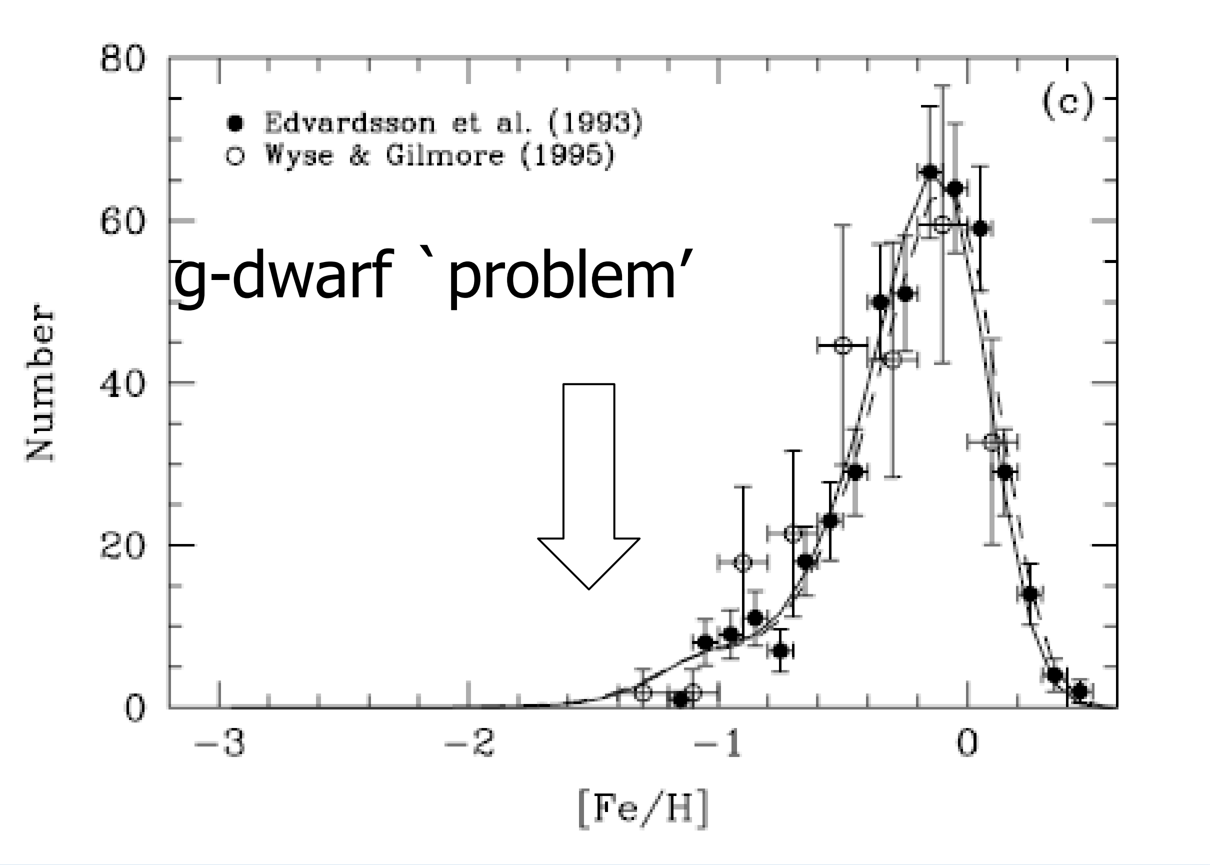

“non-standard” SN element production from zero-metal stars
➔ very high carbon abundance at low [Fe/H] is a “first star” test.

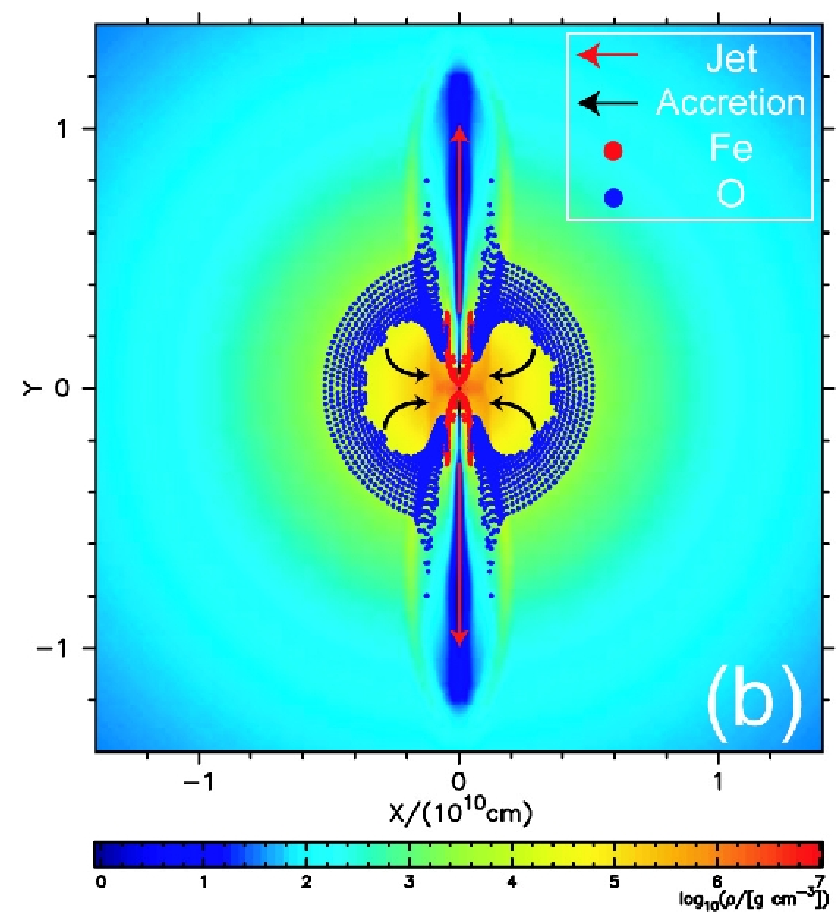

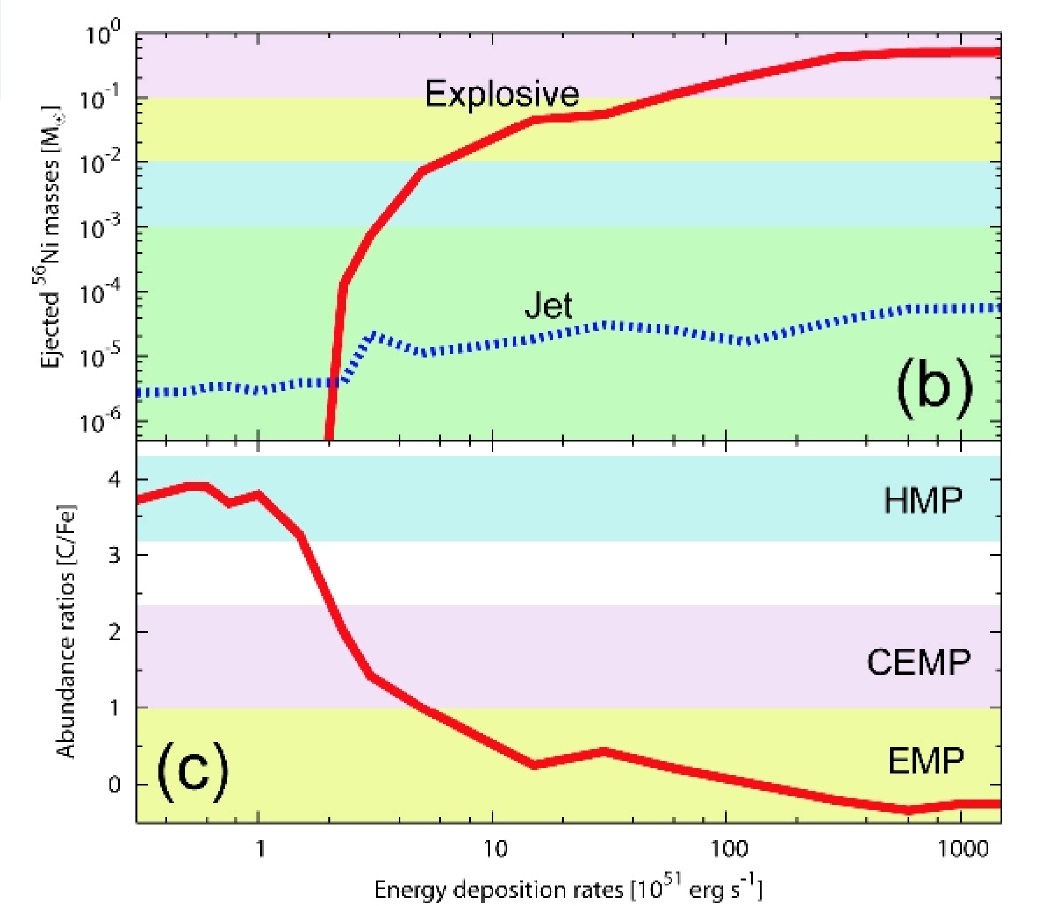

Nomoto, Komatsu, etal

A CARBON-RICH, EXTREMELY METAL-POOR (CEMP-no) STAR IN THE SEGUE 1 SYSTEM[1]

JOHN E. NORRIS[1], GERARD GILMORE[2], ROSEMARY F.G. WYSE[3], DAVID YONG[1], AND ANNA FREBEL[4]

Are these the first stars? Why are they only in the faintest dSph??

Bootes I & Segue1

[C/Fe]

versus giants in

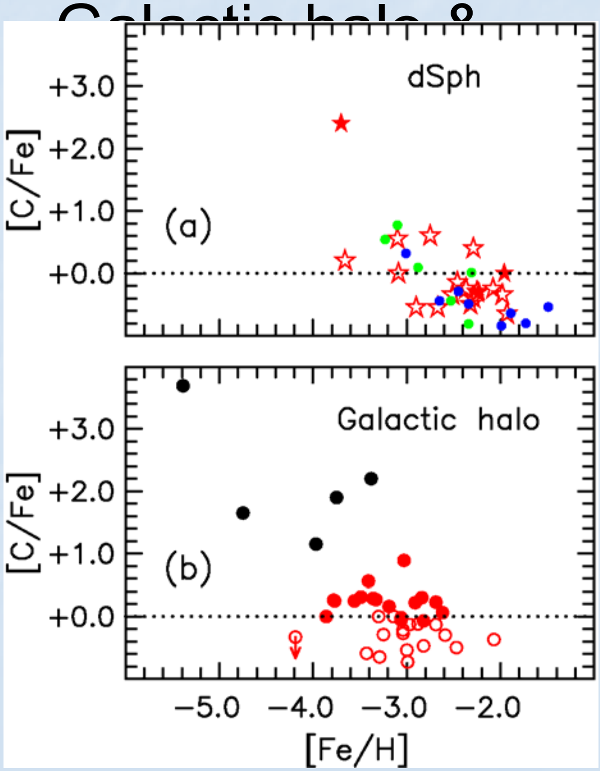

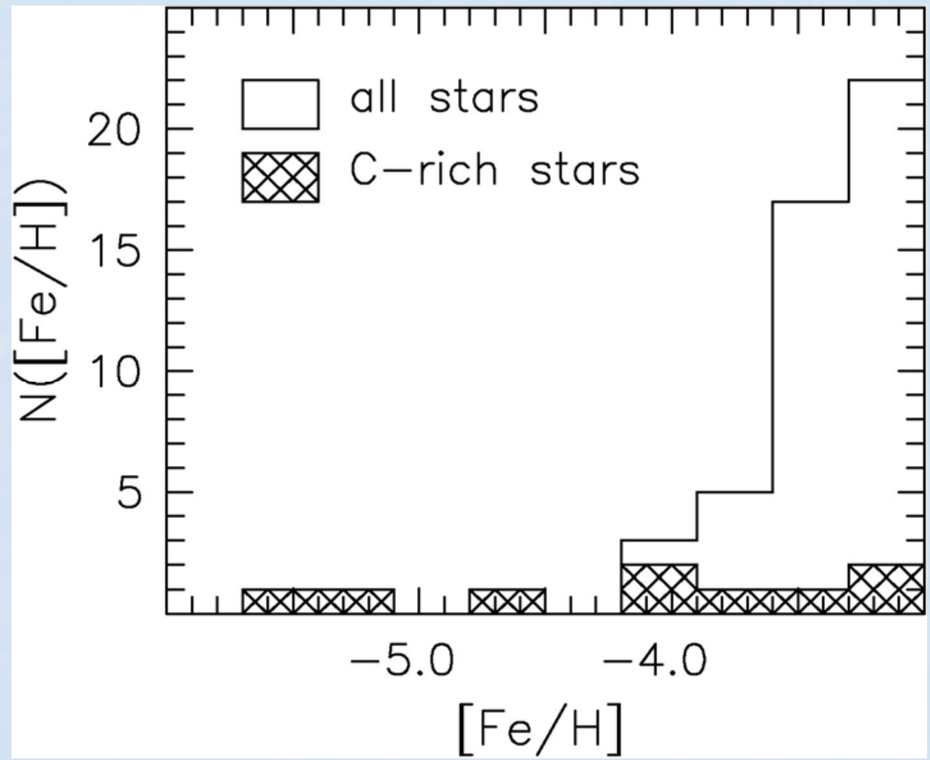

Galactic field stars

Carbon spreads in dSph – Norris, GG etal in press

Where are we with chemistry

- There is a [Fe/H] vs Mv correlation at bright magnitudes, perhaps not below Mv=-8
- There is a high abundance dispersion in dSph ➔ they really do/did have massive halos (>10^7?)
- At least the very lowest luminosity dSph have near zero-abundance stars.
- Stars in dSph are younger, have different chemistry, than halo & thick disk stars ➔ what formed the halo?
- Now on to kinematics and masses

CLAIM: all dSph have the same dark mass, variable star numbers
BUT: Very few are 300pc in size, even fewer have relevant data

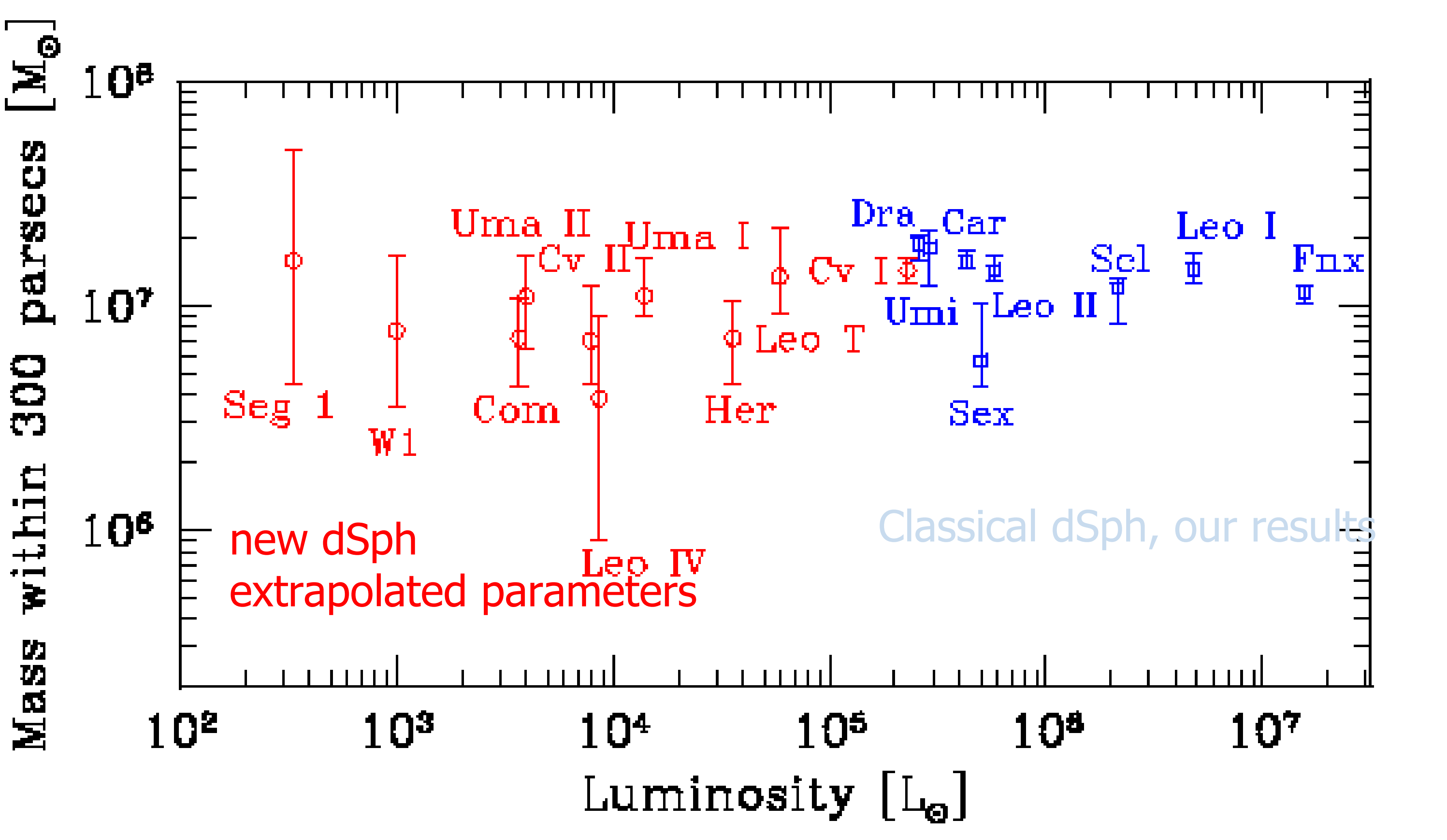

Strigari etal Nature 2008: lots of successful model explanations

Let's remove only those objects where there are no data within 50% of 300pc radiu

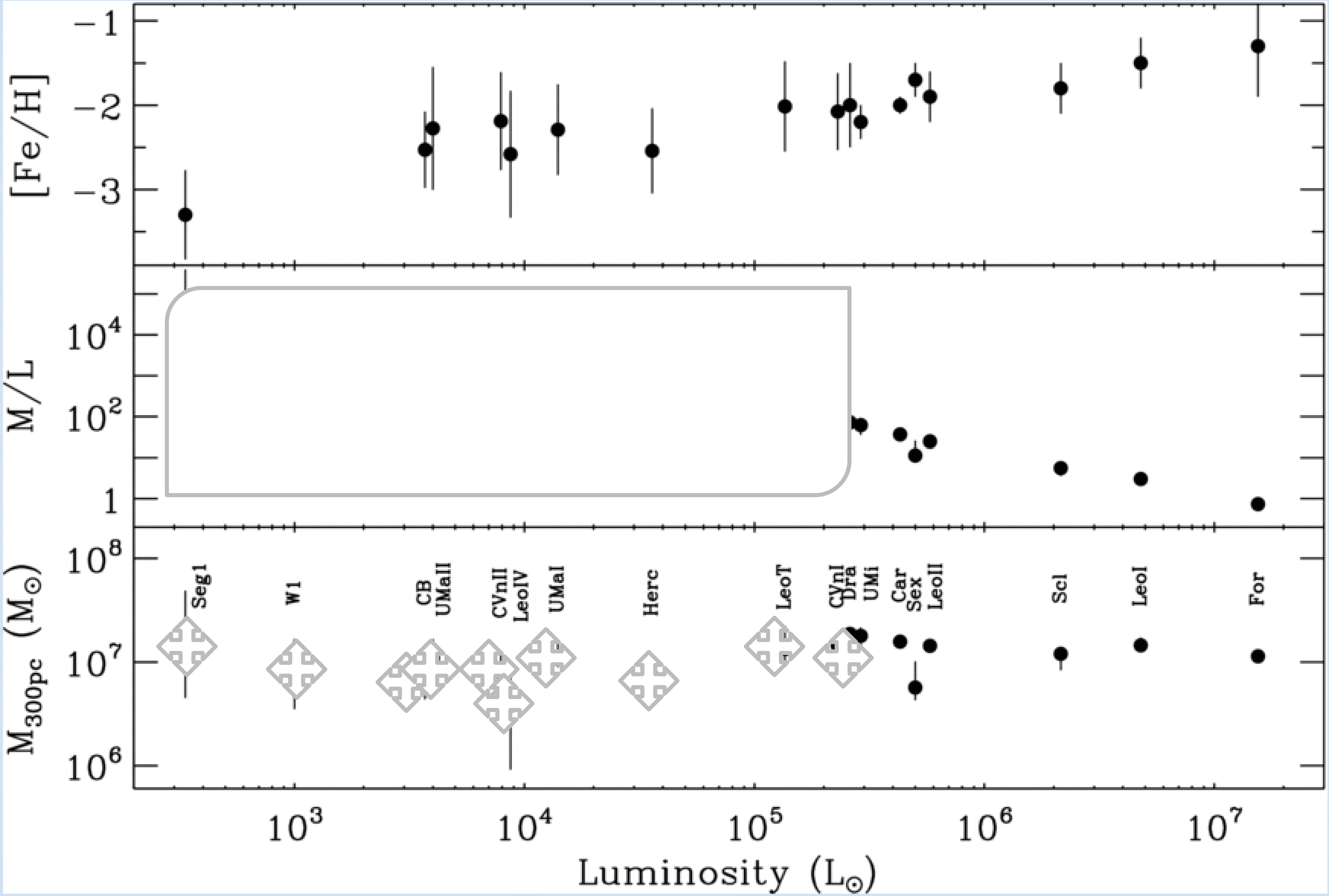

Geha etal 2009 ApJ 692 1464

Two factors to consider:
1) how good are the data?
2) How good are the analyses?

Keck kinematics by many authors, ..
“dispersion” dominated by error deconvolution

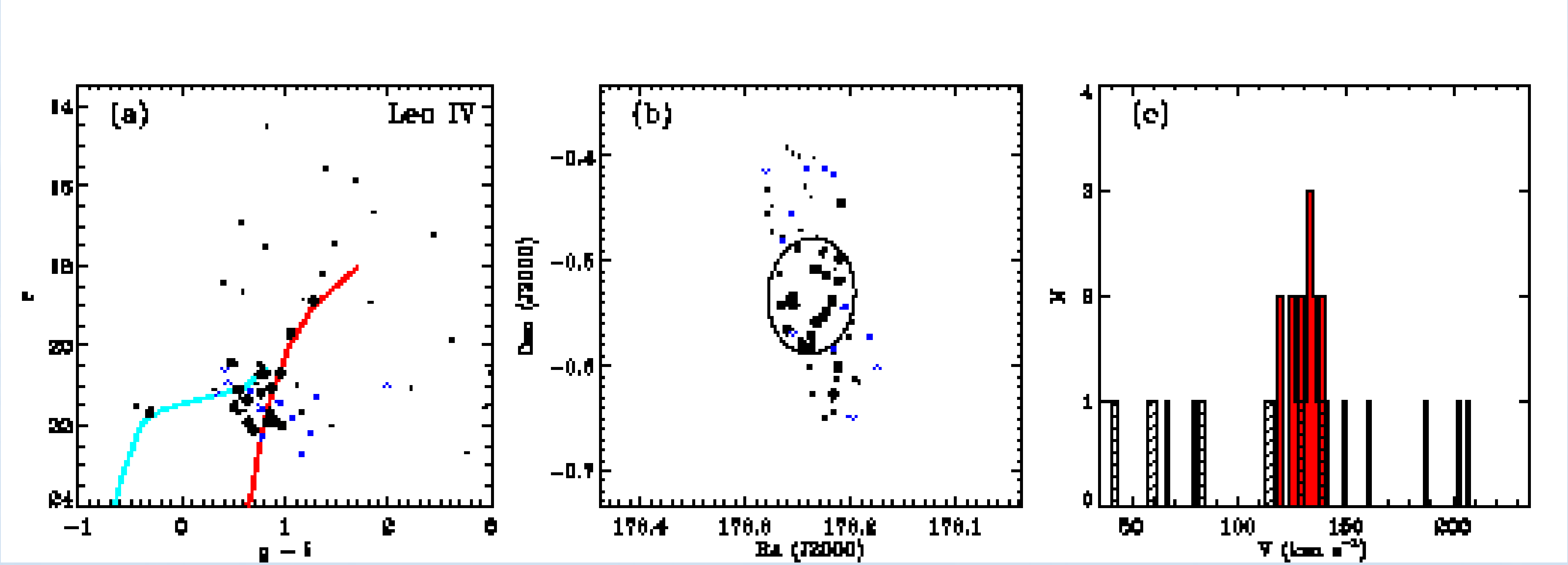

Leo-IV dispersion after errors is size of single bin in plot

Getting the most from Flames: Koposov, and IoA group
Bootes-I sample, 12 x 45min integrations

Retain full covariance: map (Gaia) models onto data, find `best` match log(g),[Fe/H], T_eff, with a Bayesian classifier.

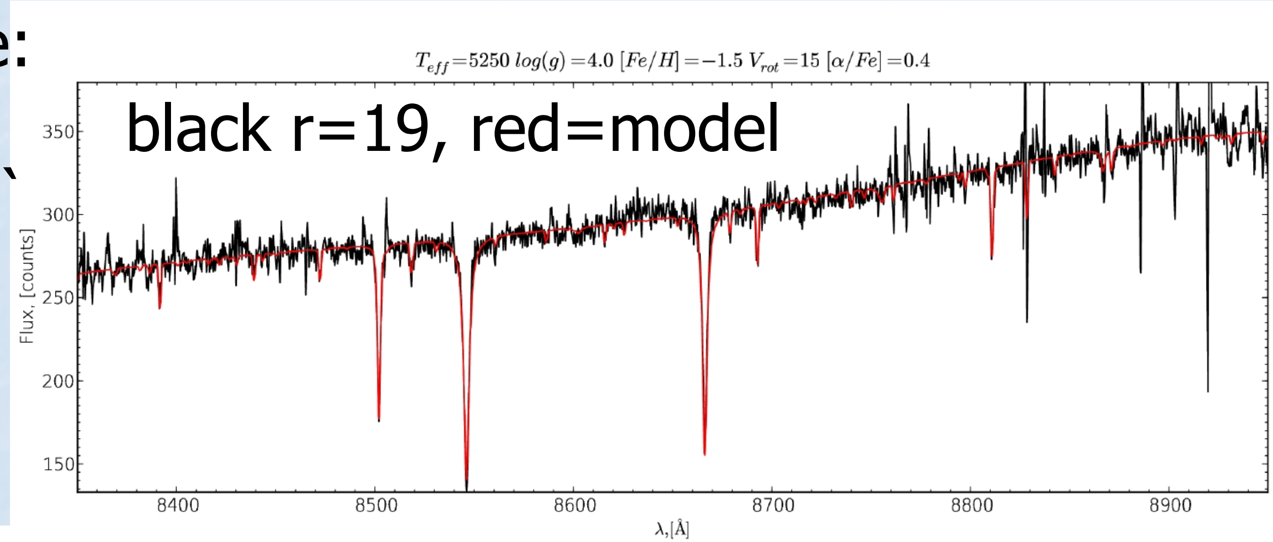

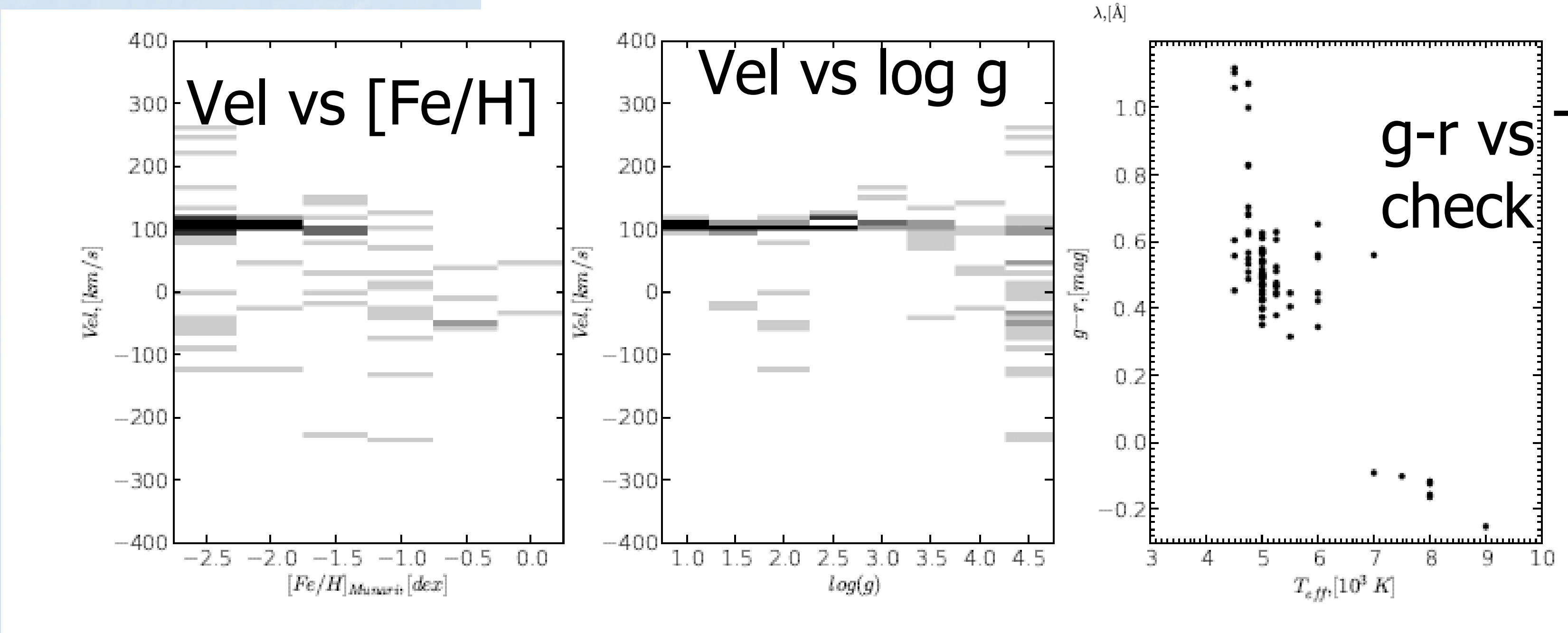

Velocity accuracy, 45m integn: vel repeats vs accuracy

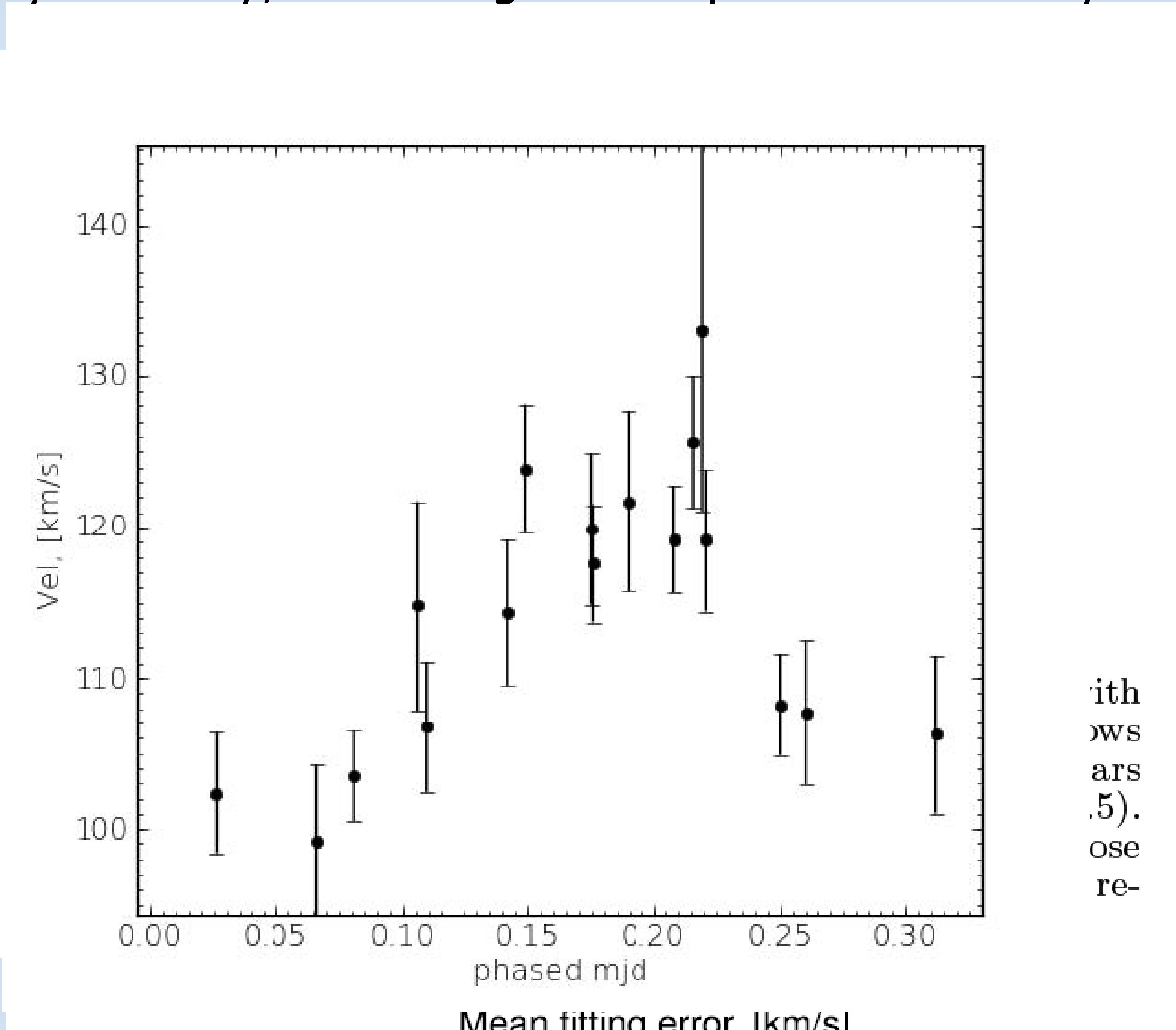

Velocity extraction uses Bayesian fitting of template families

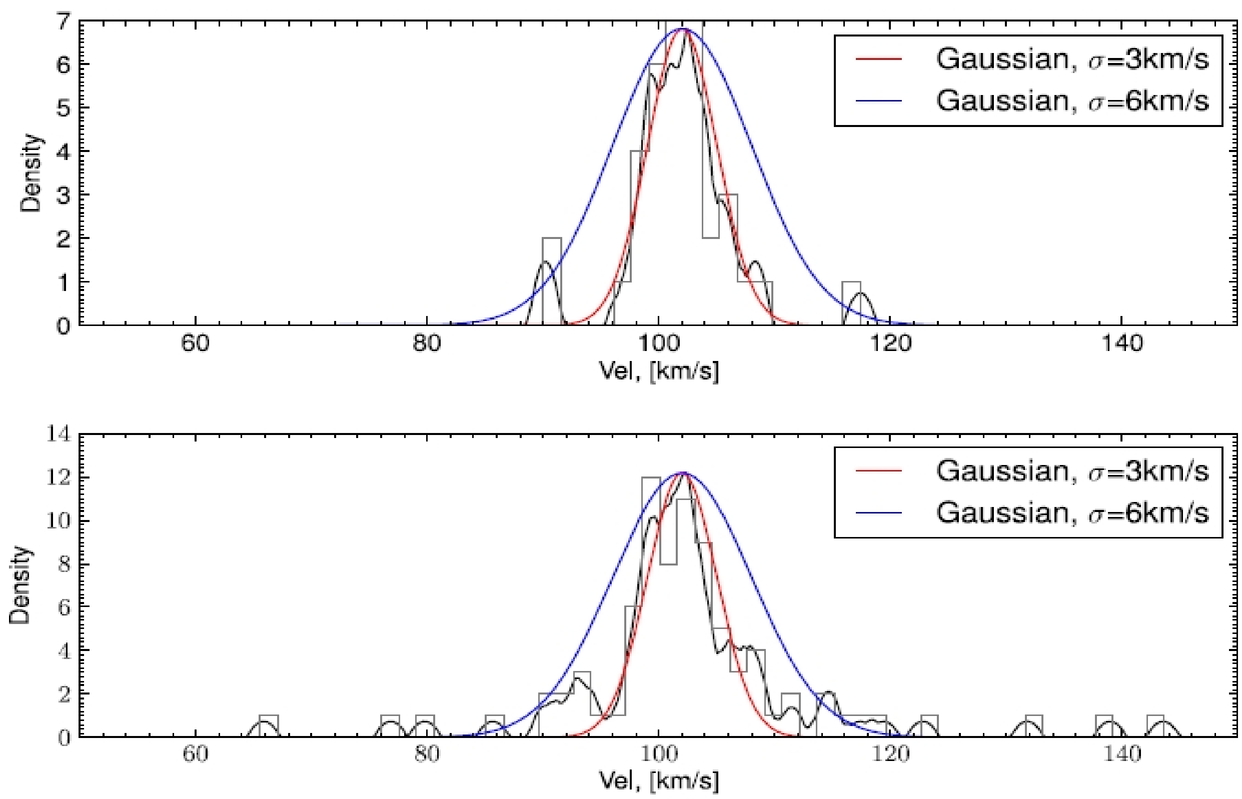

FIG. 10.— Distribution of stellar velocities. The black line shows the distribution of velocities estimated using the Epanechnikov kernel with bandwidth of 1.5km/s, grey line shows the standard histogram with the bin size of 1.5 km/s. The red and blue lines are overplotted Gaussians with sigma of 3 and 6 km/s correspondingly. The top panel shows velocity distribution for only highly probable Boo members with [Fe/H]<-1.5, log(g)<3.5, small velocity error σ_V <3 km/s and not showing significant velocity variability $log_{10}(Bayes\ factor)$ <1.5. The bottom panel show the velocity distribution for all the stars.

Summary: fishing in the dSph

- Literature kinematics of low-luminosity dSph are unreliable (as is fxcor)
- New methods of data analysis can provide

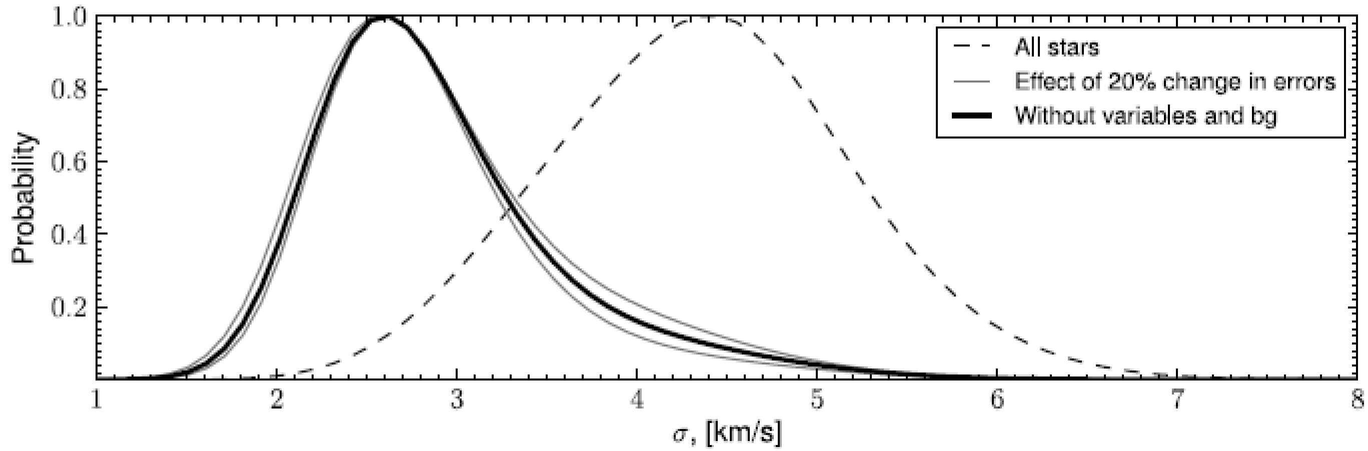

Fig. 11.— Non-normalised velocity dispersion probability distributions for different subsamples of stars. The dashed line shows the probability distribution for the velocity dispersion for all the stars, solid black line stars for not-variable stars with Fe/H]<-1.5, log(g)<3.5. The grey line shows what would happen if our error-bars on individual velocities are underestimated or overestimated by 20%

Beware underestimated errors….and non-members

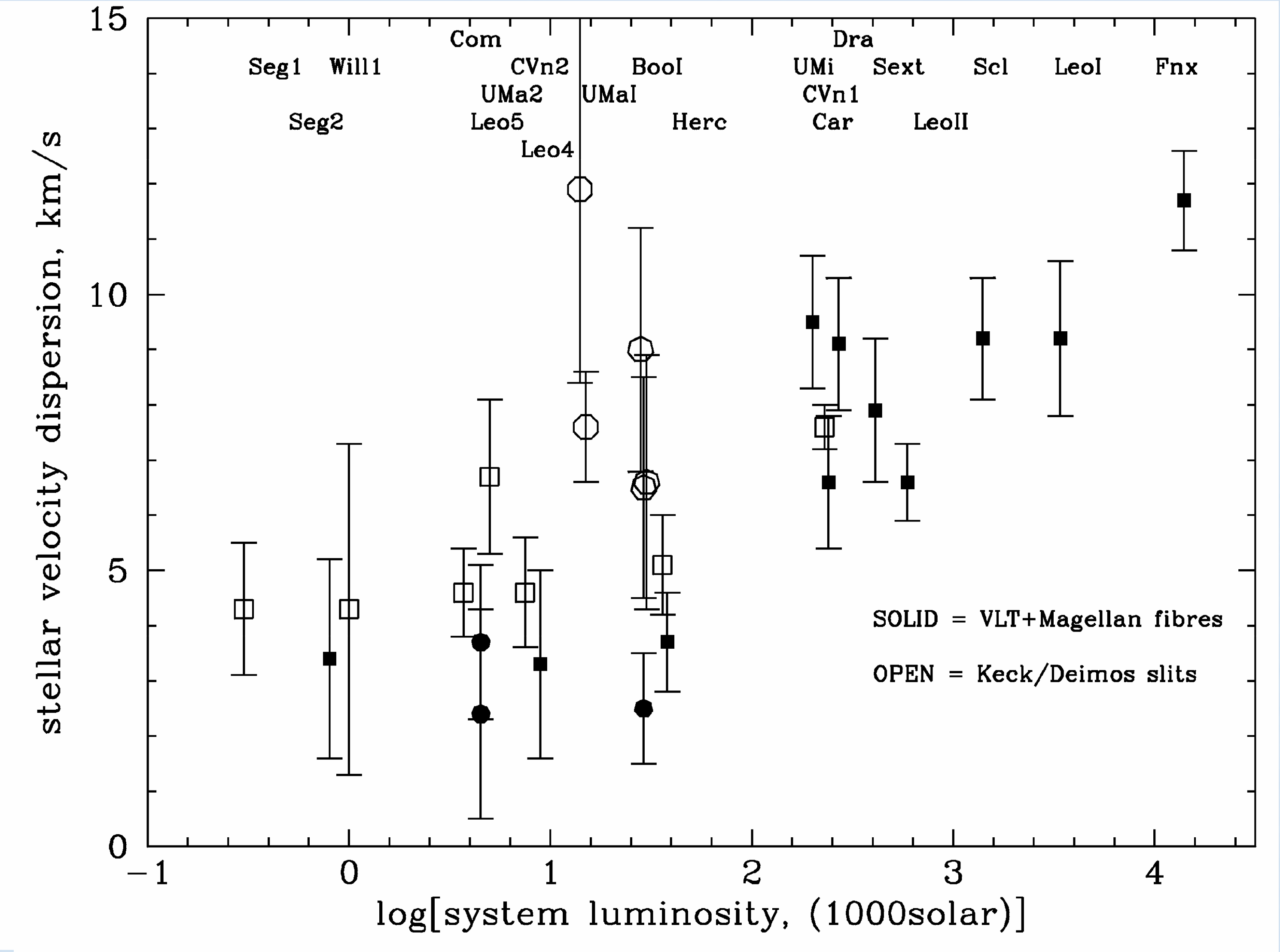

Very cold dispersions in isolated LSB galaxies are tough for MOND!

Phase space density $(\sim \rho/\sigma^3) \sim 1/(\sigma^2 r_h)$
Stellar rho increases significantly

Now lets look at the more luminous dSph, good data

M<r

- Illingworth 1976
- ....
- Mateo 1990s
- Strigari, Walker, Mamon, Wolf...

M=L?

- Mateo etal 1990s
- Wilkinson etal 2002
- Koch etal
- Lokas
- Many more

M(r)

- MB, BE, FD, RJ....
- Eddington, Jeans, Fricke, Chandrasekhar, Miyamoto, Nagai, Toomre, Lynden-Bell, Dehnen, deZeeuw, Evans, Kent &Gunn, Merrifield & Kent, Kuijken & Gilmore, Wilkinson & KEG, Wu & Tremaine, Lokas.....

Plus proxy methods based on internal abundance dispersion

Velocity dispersion profiles

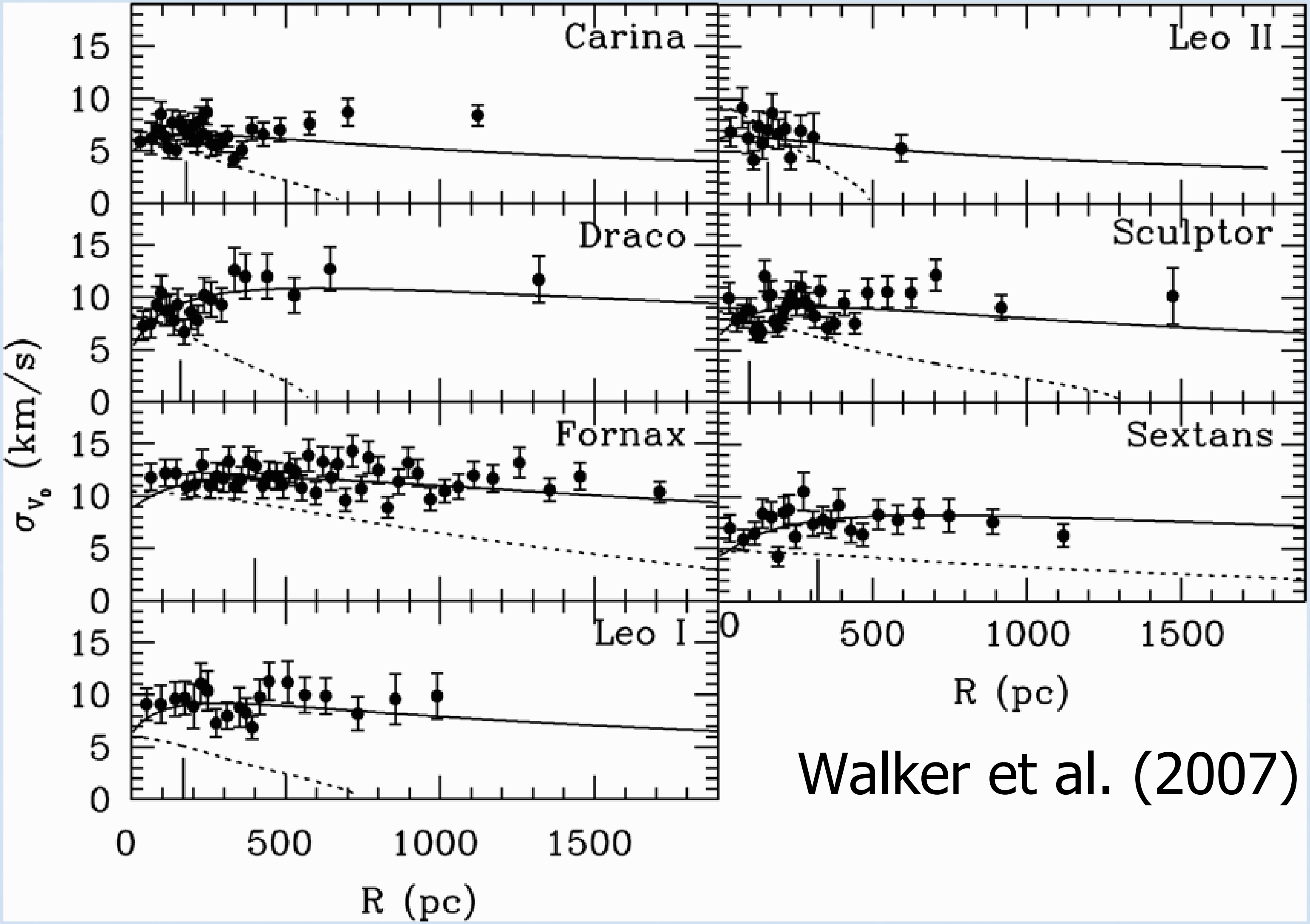

Walker et al. (2007)

dSph dispersion profiles generally remain flat to large radii

Very large precision kinematics now exist – vastly superior to the best rotation curves for gas-rich systems.
Large samples even after population selection: metal-poor

Members:
Fornax: 2737
Sculptor: 1368
Sextans: 441
Carina: 1150
Plus new VLT

Yield:
Car, Sext ~50%
For, Scl ~80%

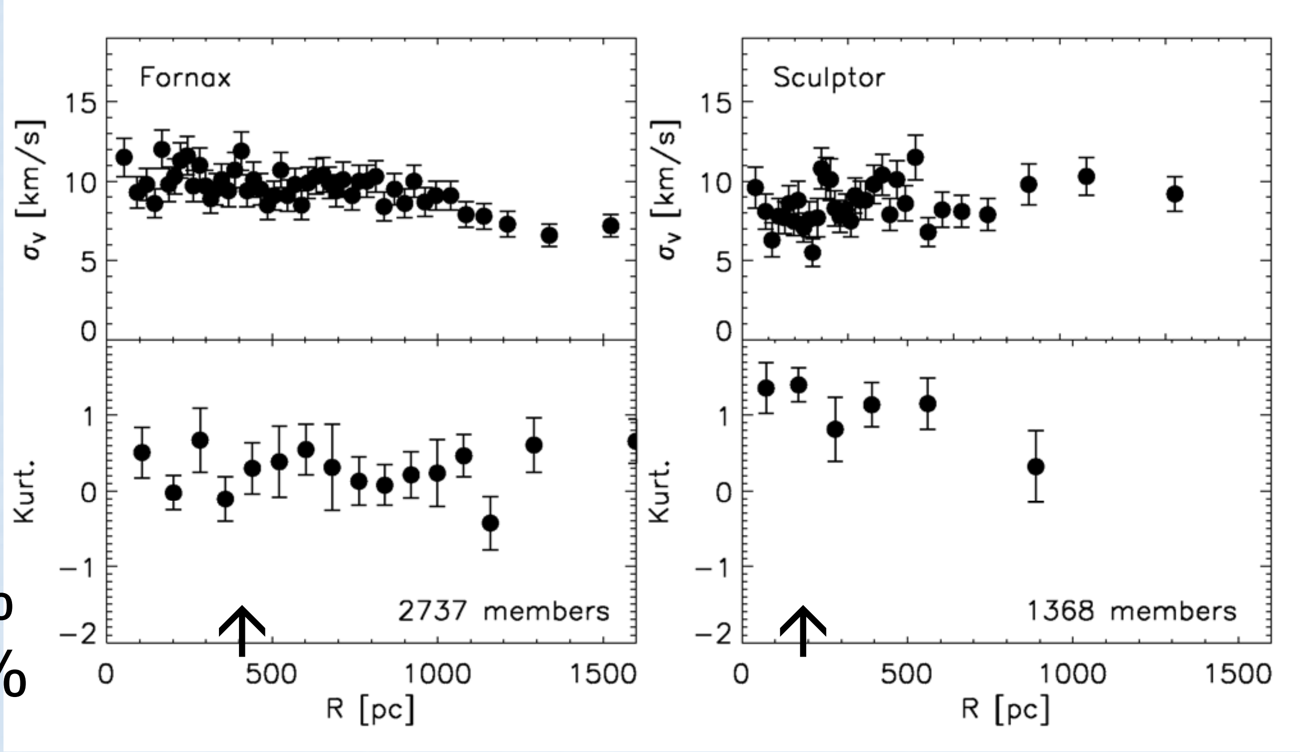

Magellan (walker etal) +VLT (Gilmore et al)

Non-members:
Wyse et al 2006

NB: with good data many galaxies are messy

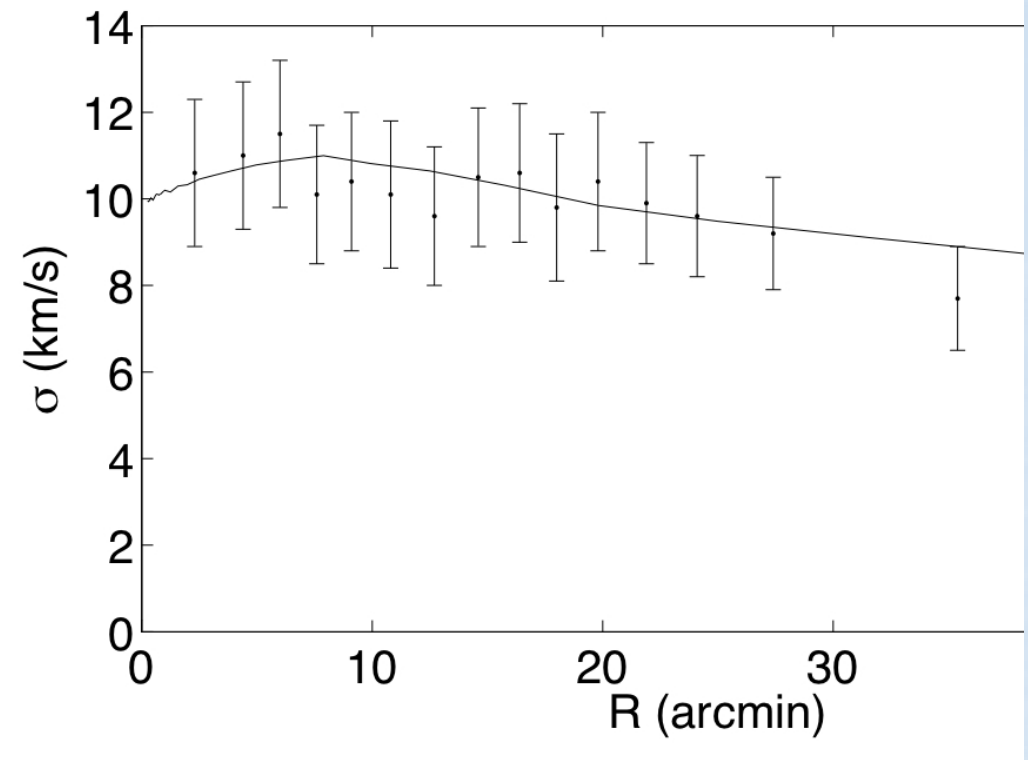

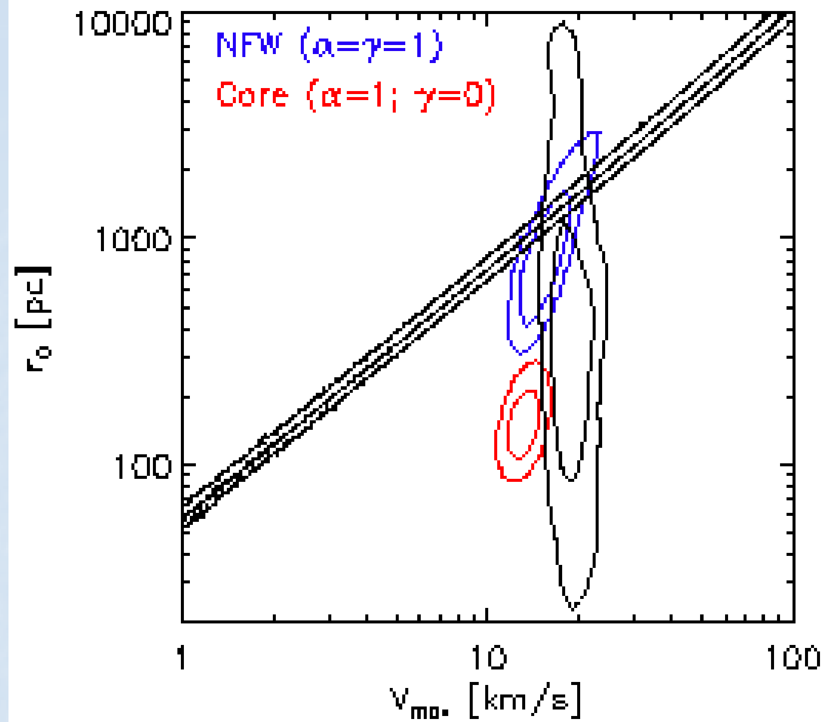

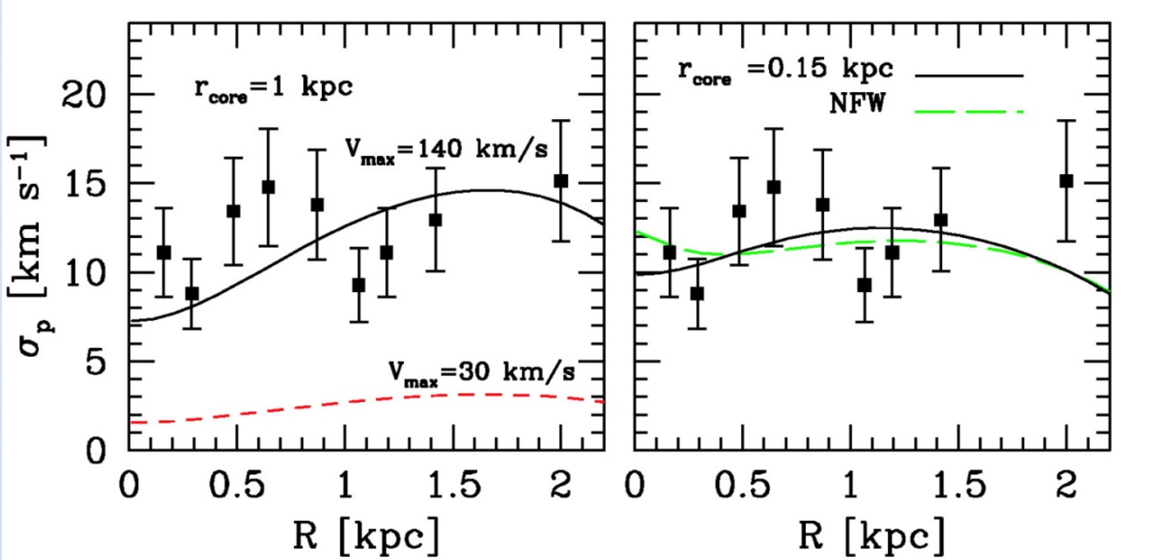

Note the data quality improvement:
First declining dispersion profile
➔ V_max=20+/-4 km/s

Top Walker etal 2009
Lower Strigari etal 2006 fit to Walker etal 2006

Fitting dSph dispersion profiles: Leo I

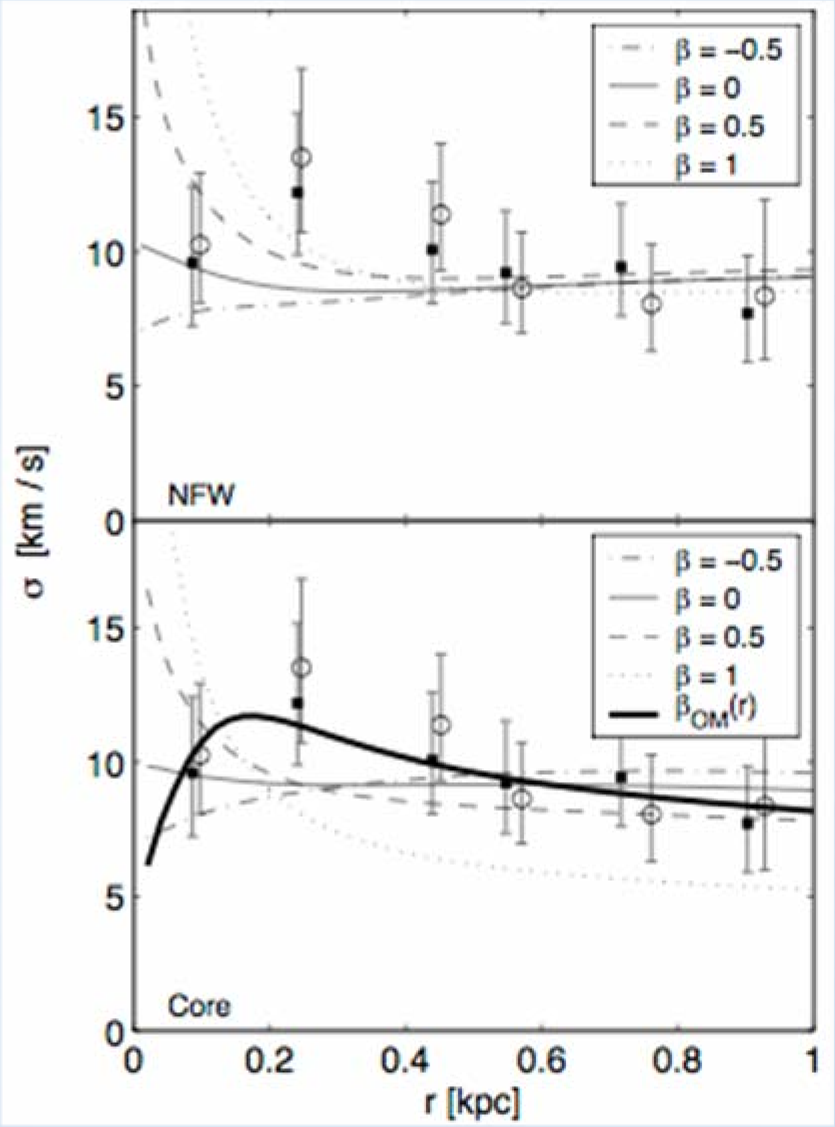

- Assume either NFW halo (1 free halo parameter) or generalised Hernquist profile (4 free halo parameters)
- Fit binned dispersion profile using Jeans equations
- Assumptions: spherical symmetry, equilibrium, restricted form for anisotropy
- Cored and cusped halo profiles fit almost equally well

Koch, GG, et al. (2007)

Core properties: adding anisotropy

Koch, GG, et al 07
AJ 134 566 '07

Fixed β   Radially varying β

Leo II

$$\beta = 1 - \frac{\langle v_\theta^2 \rangle}{\langle v_r^2 \rangle}$$

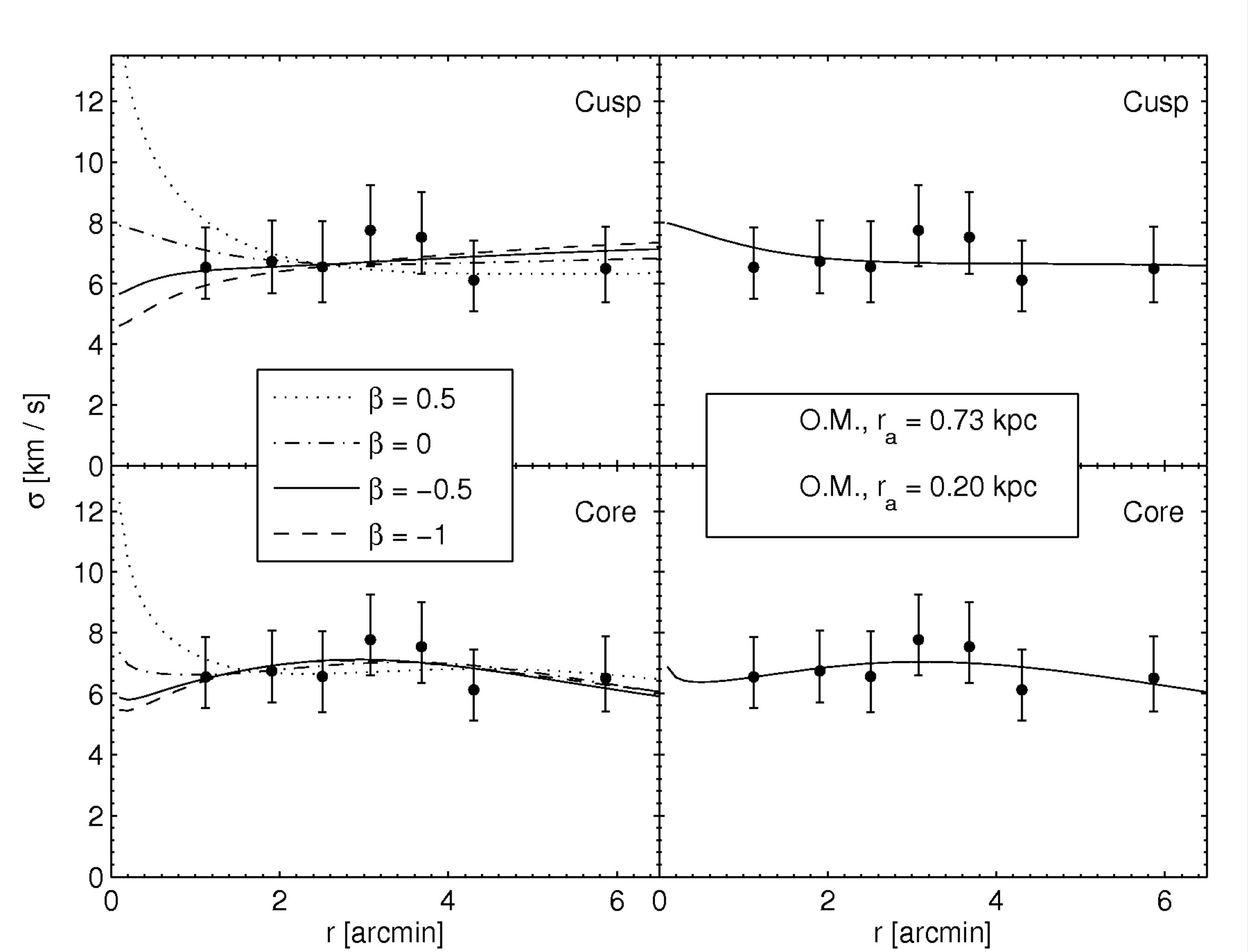

Core slightly favoured, but not conclusive

Full velocity distribution functions: breaking the anisotropy-mass profile degeneracy

Abandon Jeans $M(r) = -\frac{r^2}{G}\left(\frac{1}{\nu}\frac{\mathrm{d}\nu\sigma_r^2}{\mathrm{d}r} + 2\frac{\beta\sigma_r^2}{r}\right)$ ✗

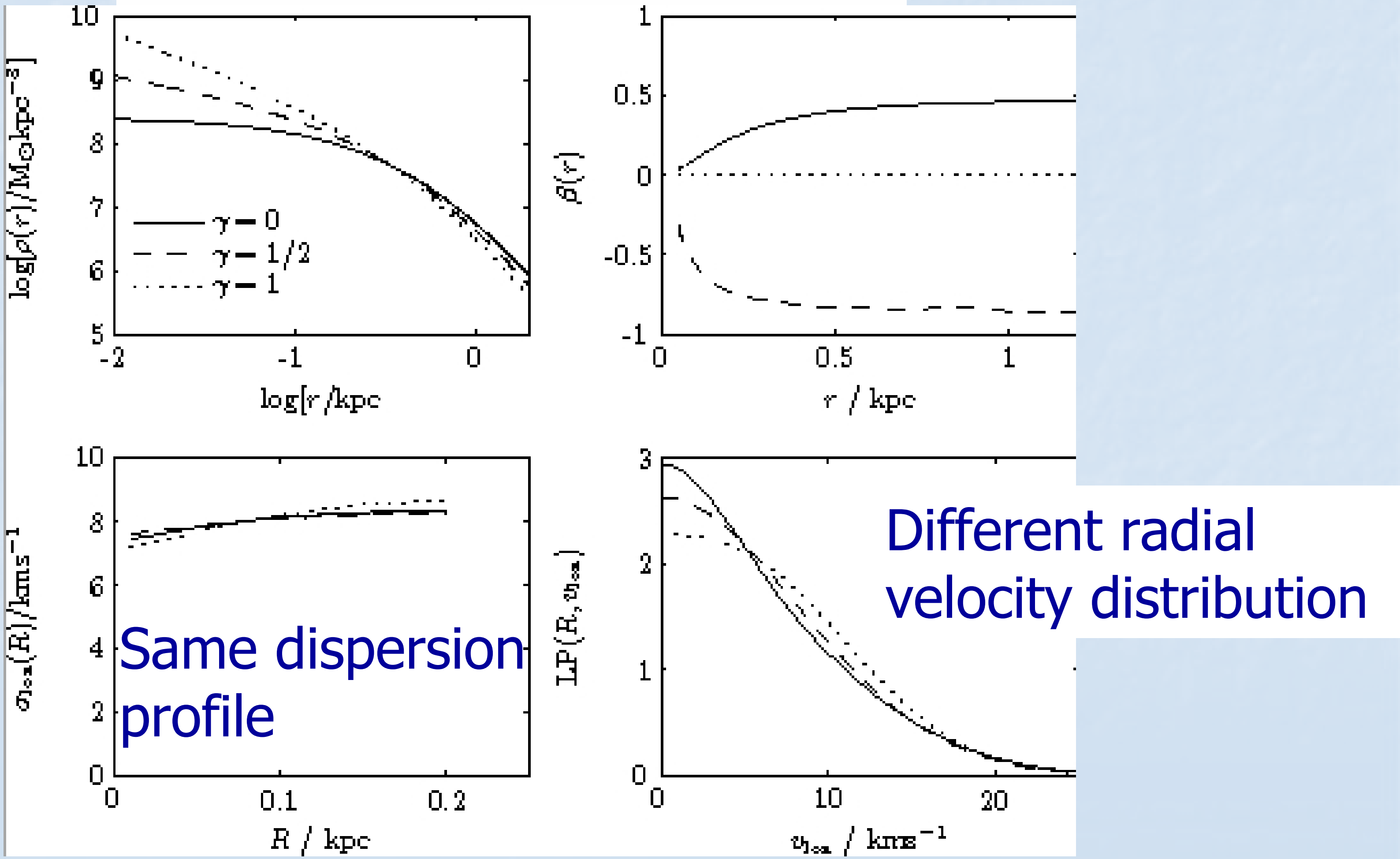

Mass measurements: DF models

This is classical physics – eg Kent & Gunn 1982

$$f_1 = A_1(e^{-E/\sigma^2} - 1)e^{-J^2/2J_0^2}, \quad (2a)$$

$$f_2 = A_2(-E)^{\beta} e^{-J^2/2J_0^2}, \quad (2b)$$

$$f_2 = A_3(e^{-E/\sigma^2} - 1)J^{-\gamma}, \quad (2c)$$

$$f_4 = A_4(-E)^{\beta} J^{-\gamma}. \quad (2d)$$

It is seen that these functions simply combine two possible forms each for the energy and angular-momentum dependence. For the energy dependence we allow for either a lowered Gaussian (with characteristic energy σ^2) or a polytrope (with power-law index β). For the angular-momentum dependence we allow for two extreme cases of anisotropy. The term $\exp(-J^2/2J_0^2)$ produces models with orbits that are isotropic in the center and radial at the edge; J_0 is the cutoff angular momentum. The term $J^{-\gamma}$ produces a more uniform anisotropy, and in fact yields a constant ratio of tangential to radial velocity dispersions (which depends on the parameter γ). Function f_1 is a King-Michie distribution, first introduced by Michie (1963) to describe the structure of global clusters. In the limit $J_0 \to \infty$ the isotropic King (1966) models are recovered. The isotropic forms of either f_2 or f_4 ($J_0 \to \infty$, $\gamma \to 0$) yield standard polytropes of index $n = \beta + 3/2$ (Chandrasekhar 1939).

cf Kuijken & Gilmore (1989) for application to local DM density

cf Wu & Tremaine 2006
Wu 2007
Lokas 2002, 2005
Wilkinson etal 2002
for dSph applications

(Very) New models

Assumptions:

- Spherical symmetry
- Tested on tri-axial N-body models - OK
- Equilibrium: tested by data
- Tracer surface density fit from star counts very sensitive in models, so we have extended the models to fit both star counts and kinematics simultaneously, and increased resolution to avoid interpolation ➔ expensive!

Models

$$\rho_{\mathrm{halo}}(r) = \frac{\rho_0}{\left(\frac{r}{r_{\mathrm{s}}}\right)^{\gamma}\left(1+\left(\frac{r}{r_{\mathrm{s}}}\right)^{1/\alpha}\right)^{\alpha(\beta-\gamma)}}$$

$$\Sigma_*(R) = 2\int_R^{\infty} \frac{\rho_*(r) r \mathrm{d}r}{\sqrt{r^2 - R^2}}$$

Same form used for both halo and stars, stellar parameters not fixed, but fit

Zhao model = generalised Hernquist/NFW/...

Distribution function

$$F(E,L) = w(E)g(E,L)$$ Gerhard (1991)

$$g(E,L) = \begin{cases} c + (1-c)(1-(1-x^2))^a & \text{tangential} \\ c + (1-c)(1-x^2)^a & \text{radial} \end{cases}$$

$$x(E,L) = \frac{L}{L_0 + L_{\rm circ}(E)}$$

NOTE: these are sufficiently general – the data test directly for any possible rotation/tidal torques/asymmetry...

Constructing the line of sight velocity/brightness distributions

- **Fit surface brightness data, not profile
- Use method by P. Saha to invert integral equation for DF:

$$\rho(\Phi) = \frac{4\pi}{r^2} \int_0^{\Phi} w(E)\,\mathrm{d}E \int_0^{L_{\max}} \frac{g(E,L)L\,\mathrm{d}L}{\sqrt{2(\Phi - E) - L^2/r^2}}$$

$$L_{\max} = \sqrt{2(\Phi - E)}r$$

- Project to obtain LOS velocity and brightness on a grid of R and $v_{\rm los}$
- **High resolution to avoid interpolation, convolve with individual velocity errors

Fitting the data

- Surface brightness data fitted as part of the MCMC
- Markov-Chain-Monte-Carlo [COSMO-MC] used to scan parameter space
- Parameters: 3 velocity distribution parameters (a, c, L_0
  4 halo parameters ($\alpha, \beta, \gamma, \rho_0$) for each of mass and surface brightness.
- Multiple starting points for MCMC used - chains run in parallel and combined once "converged"
- Error convolution included - using only data with

$$\Delta v_{\rm los} < 2\,{\rm km\,s^{-1}}$$

Inner luminosity profiles are important

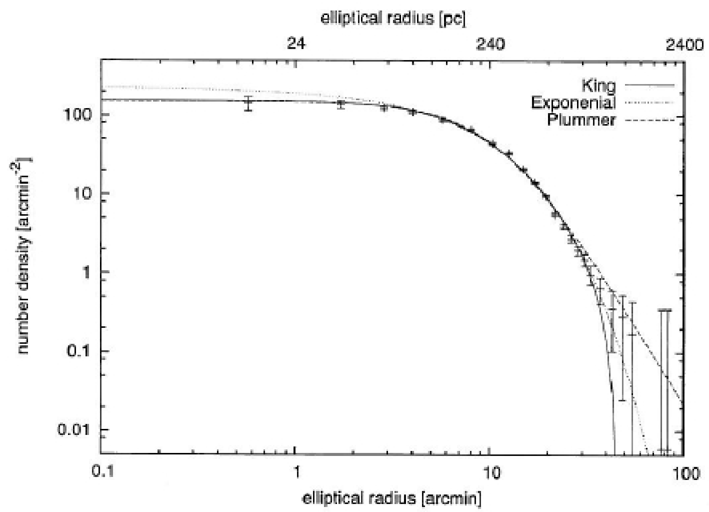

Figure 4.26 The radial profile derived by calculating the average number density within elliptical annuli. Foreground and contamination within the selected member region in panel (a) of Figure 4.24 is estimated as 0.09 arcmin^{-2} from the reference CMD and subtracted from the profile.

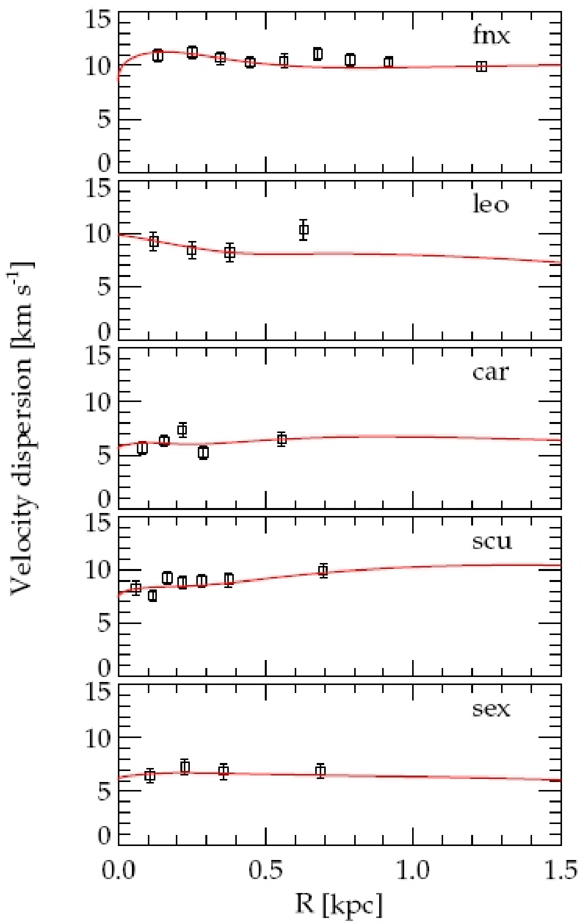

Figure 2. Line-of-sight velocity dispersion for our five satellites. The solid curves show the dispersion predicted by inserting the potential determined from the best fitting Aquarius subhalo and the photometric profile of Table 1 into Eq. 1, assuming no velocity anisotropies. The symbols show the observational data taken from Mateo et al. (2008) (Leo I) and Walker et al. (2009) (Fornax, Carina, Sculptor, and Sextans). The errors on the velocity dispersion in each bin are assigned according to Eq. 9.

Spatial resolution is an important factor

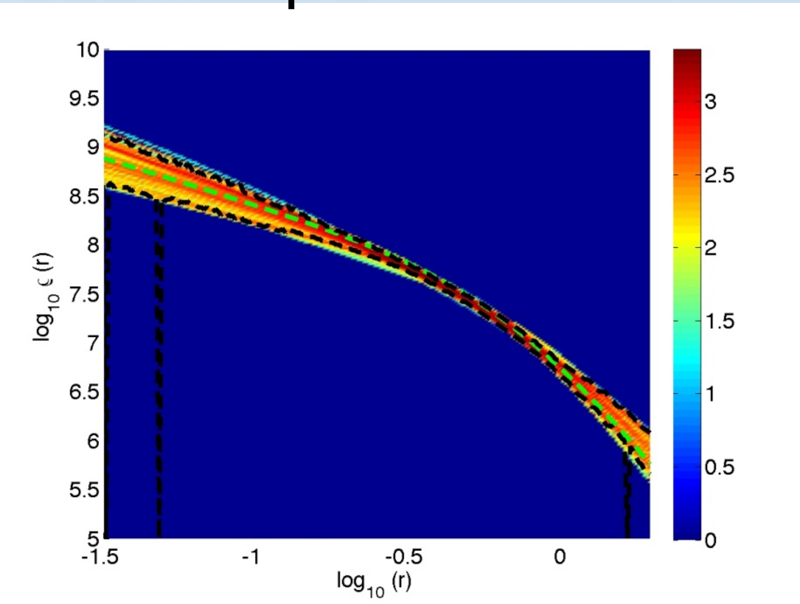

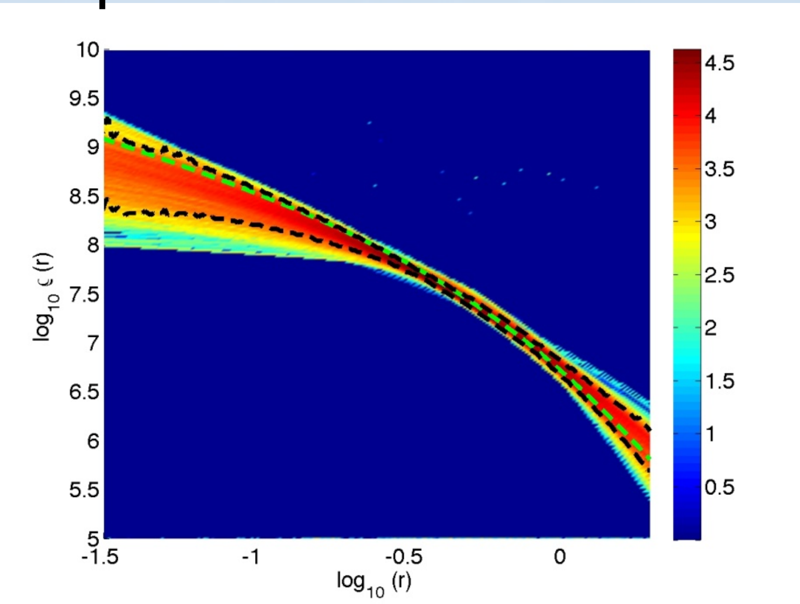

Fitting, not fixing, the surface tracer distribution is important

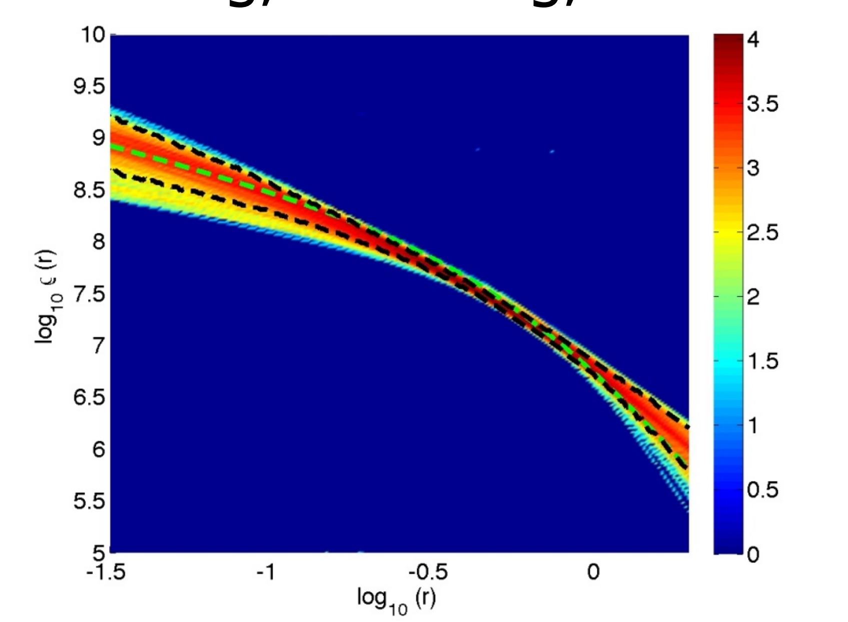

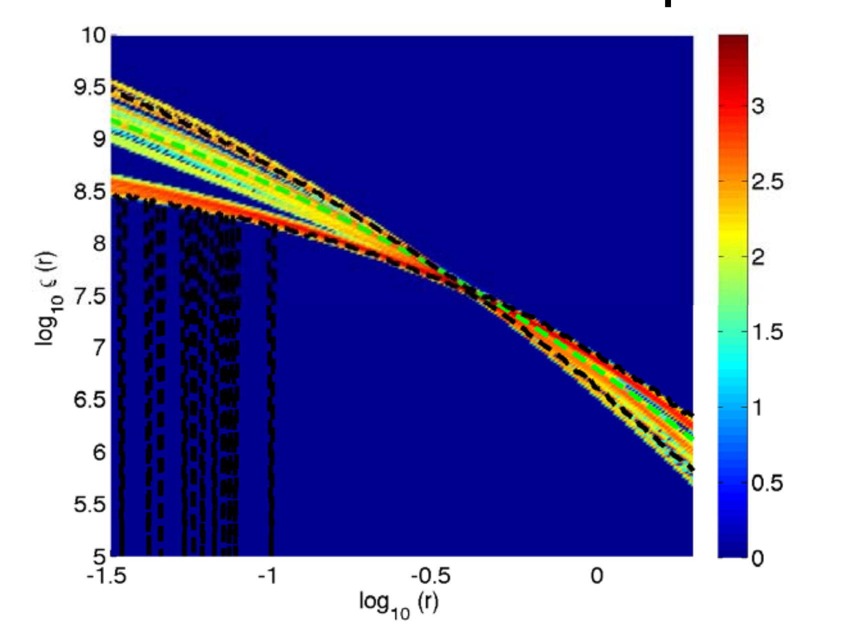

Tests with spherical models

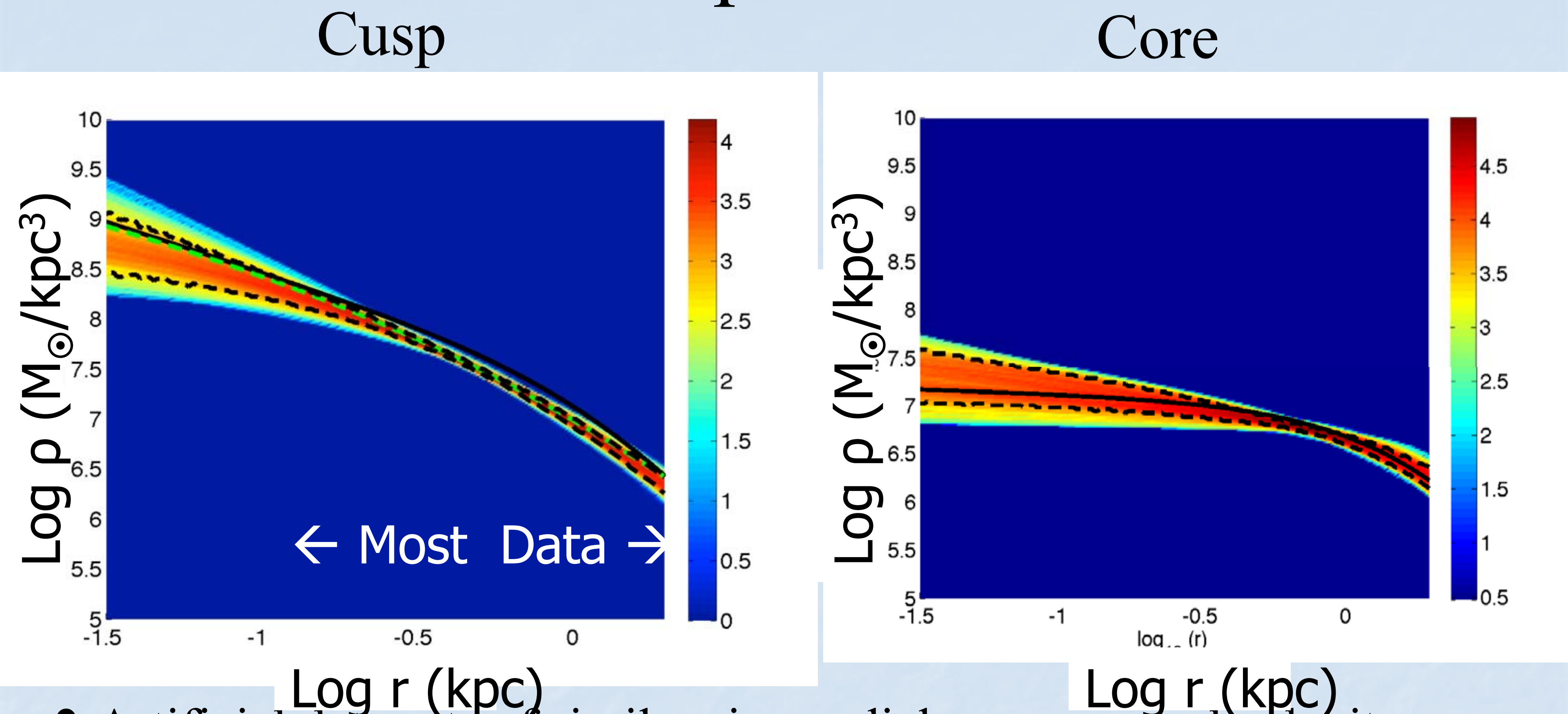

- Artificial data sets of similar size, radial coverage and velocity errors to observed data set in Fornax
- Excellent recovery of input profiles (solid black), even in inner regions; green dashed is most likely, black dashed enclose 90% confidence limits

Tests with (anisotropic) triaxial models

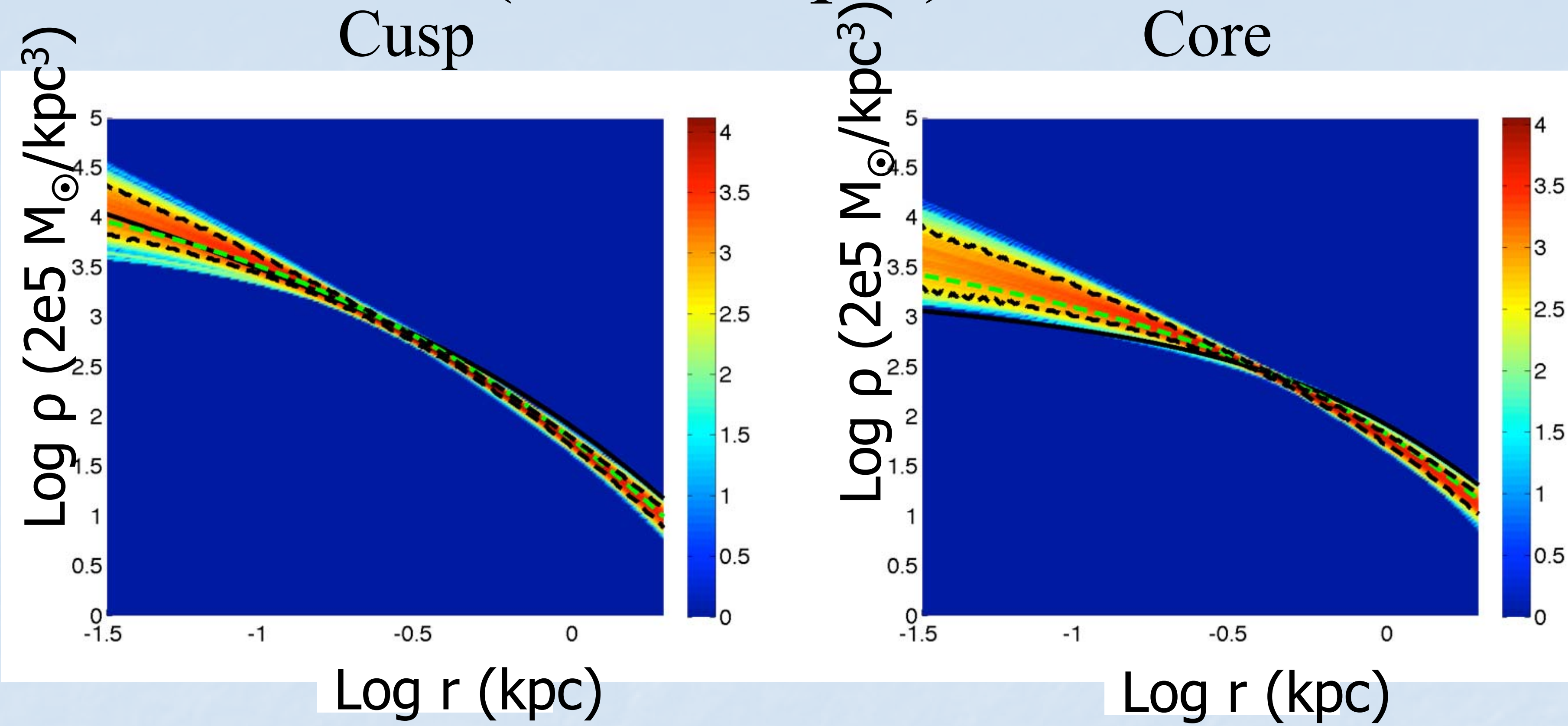

- Axis ratios 0.6 and 0.8, similar to projected 0.7 of Fornax dSph; ~2000 velocities, to match data.
- Models have discriminatory power *even when modelling assumptions not satisfied. We have a statistical test to identify where/when models fail.*

Fornax - PRELIMINARY profiles real data

Density

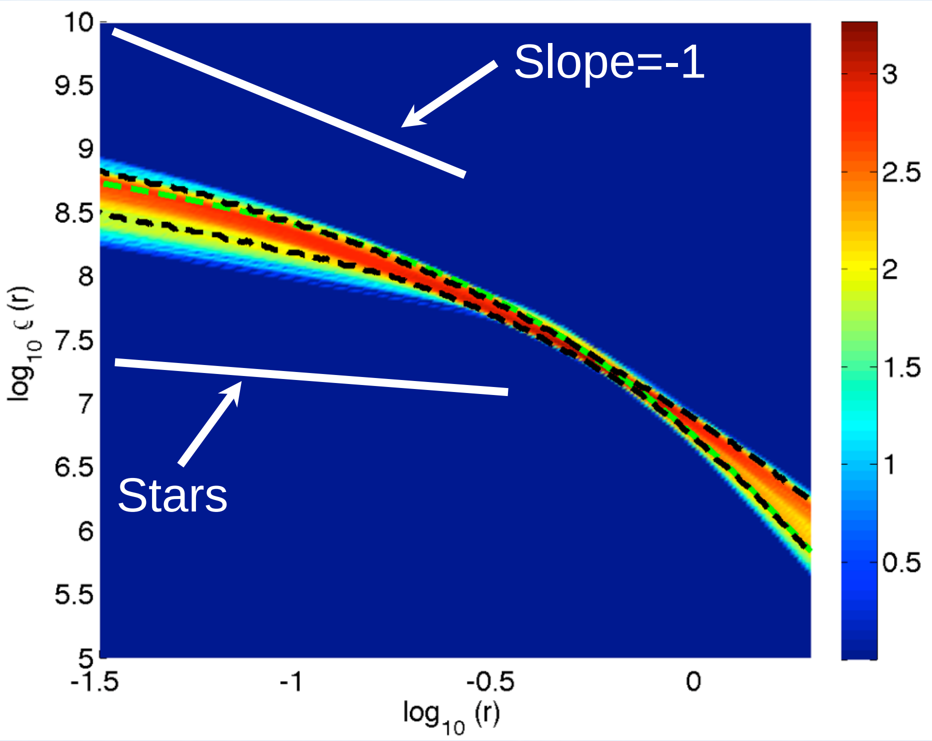

Mass

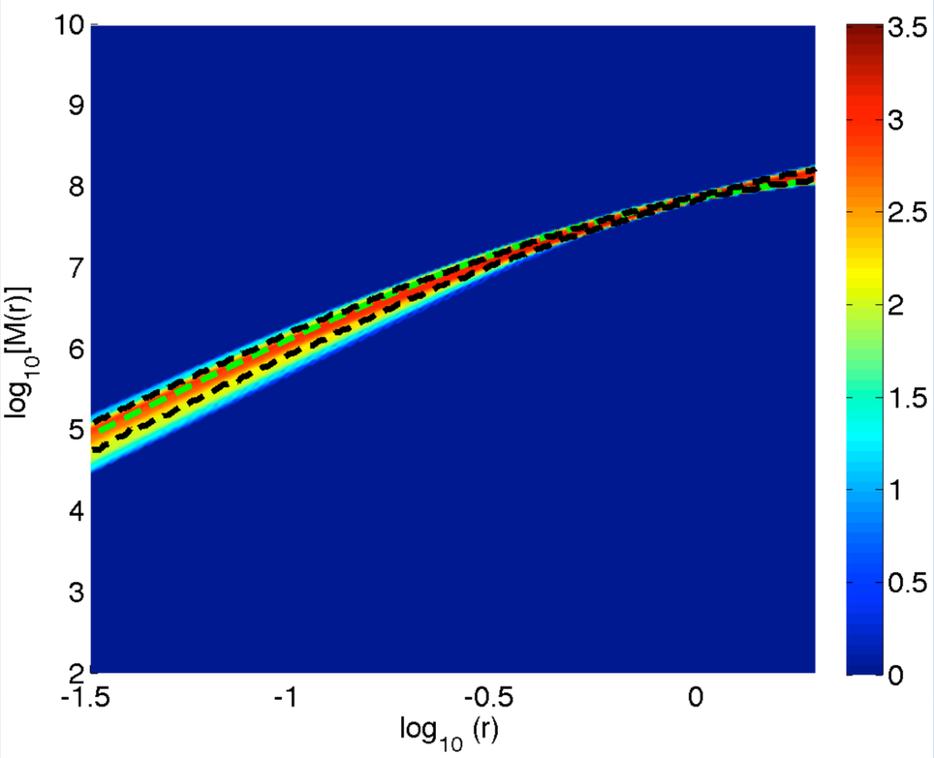

- 3 MCMC chains combined: total of ~5000 models
- At radii where most of data lie, clear constraints on profile
- baryonic mass included, of course!

Fornax - dispersion profile

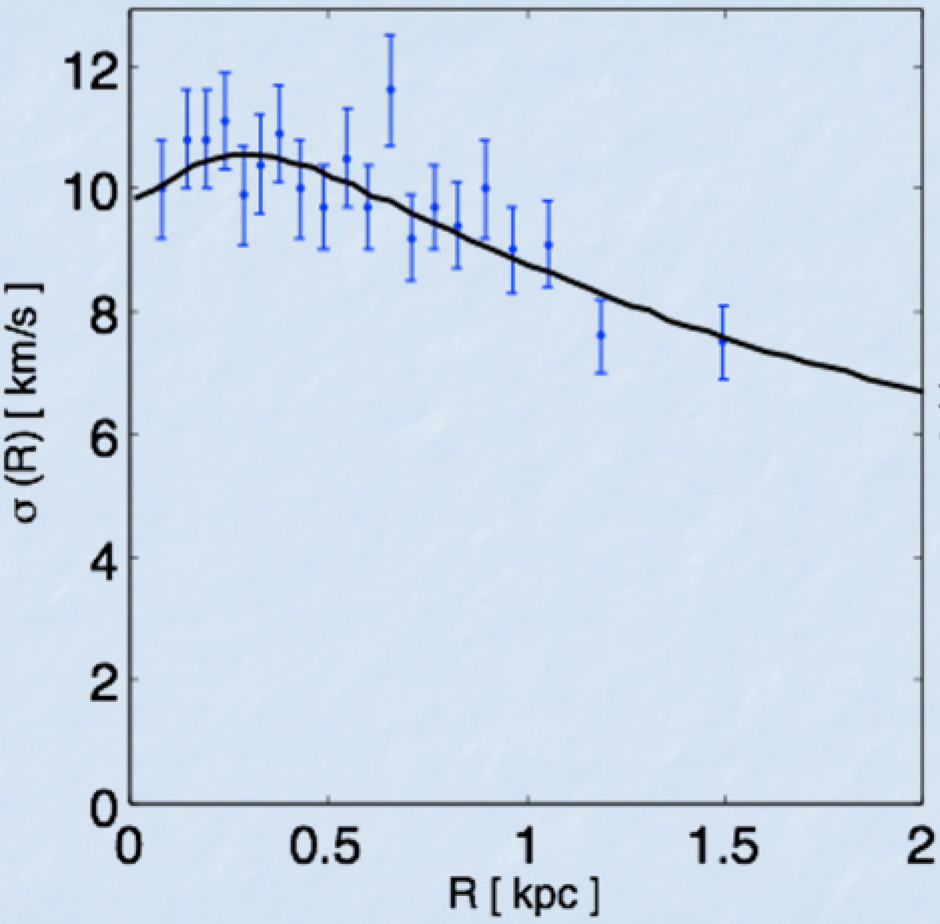

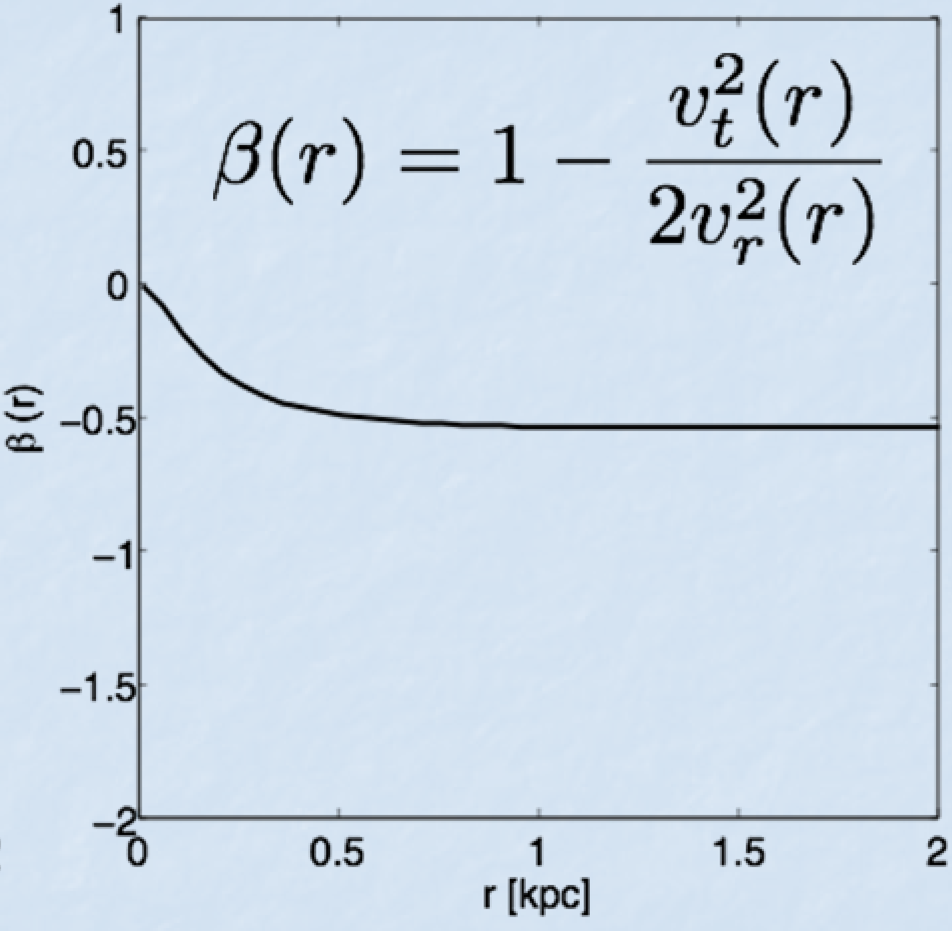

NB: Dispersion data not used to constrain models

Summary:

- A minimum physical scale for galaxies:

  half-light radius >100pc

  - mass size scale somewhat larger (x2?)

- Cored? mass profiles, with similar low mean mass densities

  $\sim 0.1 M_{\odot}/pc^3$, ~10GeV/cc

  - phase space densities fairly constant, maximum for galaxies – are they the first halos?

Pre-Galactic abundances in lowest-luminosity

" Examine the objects as they are and you will see their true nature; look at them from your own ego and you will see only your feelings; because nature is neutral, while your feelings are only prejudice and obscurity."

邵雍, *Shao Yong*, 1011–1077

Eddington analysis of kinematics: spherical, isotropic, assume NFW
Strigari, White, Frenk 2010

Table 1. Note that since our goal is to demonstrate that the observations are consistent with simple spherical, isotropic models within ΛCDM subhalos, it is not necessary for us to choose the best-fit profile parameters; rather we need only show that the parameters we do choose are consistent with the star count data.

Table 2. KS probabilities for the maximum difference between the observed and modeled cumulative distributions of $|v_{\rm i}|$ within four equally populated annuli in each of our observed satellites. Bins 1-4 correspond to the annuli of Fig. 4 ordered from inside to outside. The complement of each of these values represents the

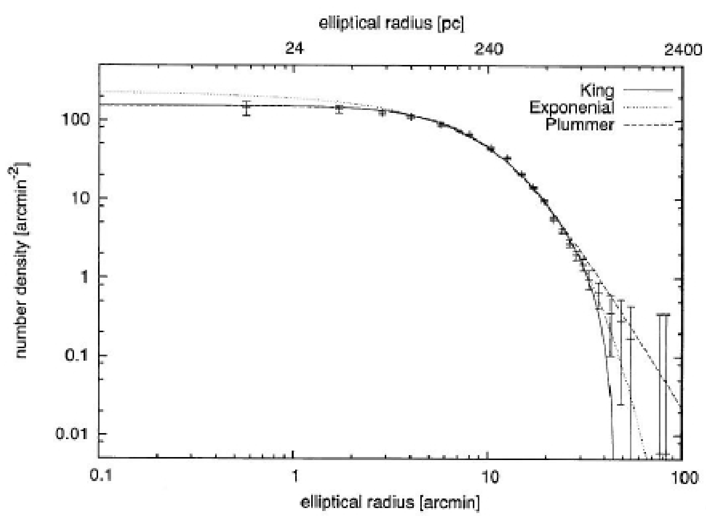

Figure 4.26 The radial profile derived by calculating the average number density within elliptical annuli. Foreground and contamination within the selected member region in panel (a) of Figure 4.24 is estimated as 0.09 arcmin^{-2} from the reference CMD and subtracted from the profile.

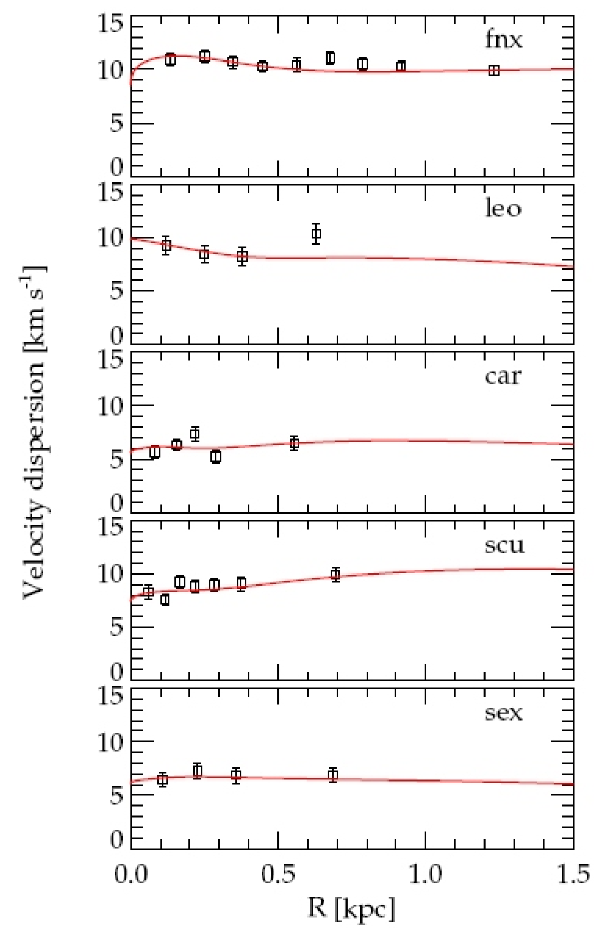

Figure 2. Line-of-sight velocity dispersion for our five satellites. The solid curves show the dispersion predicted by inserting the potential determined from the best fitting Aquarius subhalo and the photometric profile of Table 1 into Eq. 1, assuming no velocity anisotropies. The symbols show the observational data taken from Mateo et al. (2008) (Leo I) and Walker et al. (2009) (Fornax, Carina, Sculptor, and Sextans). The errors on the velocity dispersion in each bin are assigned according to Eq. 9.